HEART FAILURE REMODELING AND VENTRICULAR ARRHYTHMIA: THE ROLE OF ALTERED L-TYPE CALCIUM CHANNEL FUNCTION IN THE DEVELOPMENT OF LETHAL ARRHYTHMIAS

by
Alexandra D. Loucks

A thesis submitted to Johns Hopkins University in conformity with the requirements for the Master's degree in Biomedical Engineering.

Baltimore, Maryland
December, 2018

Abstract

Heart failure (HF) is one of the most common causes of morbidity and mortality worldwide. Although many patients suffering from HF die from sudden cardiac death caused by arrhythmias, the mechanism linking HF remodeling to an increased arrhythmogenic propensity remains incomplete. Independently of the etiology of the disease, HF is typically characterized by a progressive loss of transverse tubule (T-tubule) domains, which leads to an altered distribution of L-type Calcium channels (LTCCs). Ischemic cardiomyopathy (ICM) is usually accompanied by an increase in LTCC open probability (P_o) in the T-tubules which depends on the activity of protein kinase A (PKA). In dilated cardiomyopathy (DCM) on the other hand, the increased LTCC P_o on the non-T-tubule sarcolemma results from enhanced calcium-calmodulin kinase II (CaMKII) modulation. Microdomain degradation also causes the disruption of the β_2 adrenergic receptor (β_2AR) and phosphodiesterase (PDE) signaling localizations, normally confined to the dyadic space.

The goal of this study was to analyze how these subcellular changes affect the function of LTCCs and lead to the emergence of ventricular cell-level triggers of arrhythmias. Furthermore, we aimed to compare how the two different pathways lead to different phenotypes in ICM vs. DCM.

Using computational modeling, we analyzed the behavior of the LTCC current (I_{CaL}) under basal and sympathetic stimulation and its effect on cellular action potentials (APs). Our results showed that channels redistributed from the T-tubular membrane to the bulk of the sarcolemma displayed an altered function in their new, non-native signaling domain. The changes in LTCC current led to the development of early afterdepolarizations (EADs) in both types of HF, and

triggered reentrant arrhythmias only in the DCM model.

Thus, our work shows that altered LTCC function is a potential cause for the emergence of cell-level triggers of arrhythmia, and that CaMKII, β_2ARs and PDEs present useful therapeutic targets for treatment of HF and prevention of sudden cardiac death.

Thesis Readers:

Primary Reader: Natalia A. Trayanova, Ph.D.

Murray B. Sachs Professor
Department of Biomedical Engineering
Institute for Computational Medicine
The Alliance for Cardiovascular and Treatment Innovation
Johns Hopkins University

Secondary Reader: Raymond Winslow, Ph.D.

Raj and Neera Singh Professor
Institute for Computational Medicine
Center for Cardiovascular Bioinformatics and Modeling
Department of Biomedical Engineering
Johns Hopkins University

Acknowledgements

First and foremost, it is a genuine pleasure to express my deep gratitude to my advisor, Dr. Natalia Trayanova, for her tireless guidance, mentorship and support during my time in graduate school. I want to especially thank her for pushing me out of my comfort zone, challenging me to be a better scientist and writer, and for trusting me even when I lacked faith in myself. Working with her was an absolutely wonderful experience. I owe her a great debt for grooming my scientific rationale and providing me with all the freedom needed to build a strong scientific foundation for my future endeavors.

I am also extremely thankful to Dr. Patrick Boyle, for his kind help and encouragement along this journey. His dedication and interest in helping the students from our lab, as well as his thoughtful suggestions and counsel have helped me immensely towards the completion of this thesis.

To all the members of the Computational Cardiology Lab with whom I have had the honor of working, I thank you for the fun and good memories you made possible.

Lastly, to my parents, and my beloved husband Eric, thank you. My experience would not have been the same without your unconditional love and care. I certainly wouldn't be here without them.

Contents

List of Figures

Chapter 1: Background and motivation

1.1 The Electrophysiology of the Heart

The heart is a vital organ that acts as a pump, moving blood through arteries and veins to deliver oxygen and nutrients to the rest of the body and remove carbon dioxide (Figure 1.1). The heart consists mostly of cardiac muscle (myocardium), a special type of muscle composed of fiber-like arrays of electrically coupled excitable cells (cardiomyocytes). Electrical signals in the heart function as triggers, protectors and controllers of contractions. Under normal conditions, pacemaker cells located in the sinoatrial (SA) node initiate a contraction by spontaneously generating an electrical signal. This electrical signal propagates from cell to cell in a wave-like manner, causing the upper chambers of the heart (the left and right atrium) to contract and pump blood into the relaxed lower chambers of the heart (the ventricles). From an electrical point of view, the atria are almost completely separated from the ventricles by the fibrous body of the heart. Thus, the electrical signal which originated in the atria can only reach the ventricles via the atrioventricular (AV) node and the bundle of His. The main role of the AV node is to provide a delay in electrical conduction and slow the electrical wave, allowing the ventricles to properly fill with blood before their contraction. After passing through the AV node, the electrical signal moves through the bundle of His and reaches the Purkinje fibers, a specialized network of cells which rapidly carry the electrical signal to the apex of the heart. Once the electrical excitation is transferred to the ventricular myocardium through the Purkinje ventricular junction, the wave propagates across the left and right ventricle, causing them to

contract and pump blood to the body and lungs. The whole heart then returns to diastole, until the next excitation arises from the SA node.

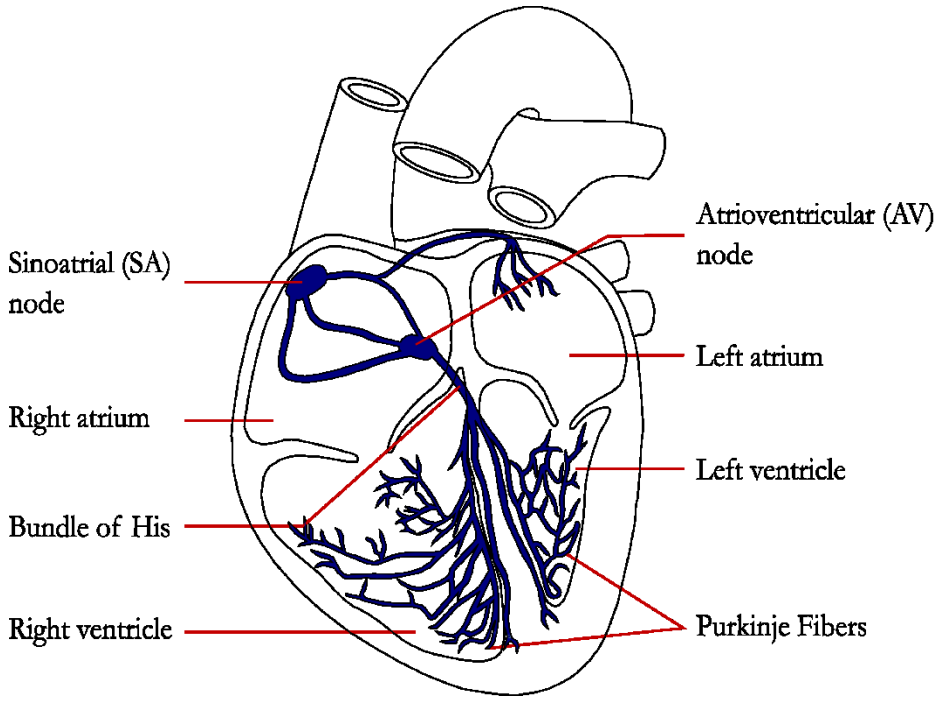

Figure 1.1 Cardiac anatomy and electrical conduction system.

1.1.1 Cardiac Action Potentials

In the heart, an electrical signal is called action potential and is defined as a rapid depolarization followed by a slower repolarization of the excitable membrane of a cardiomyocyte. This membrane, also known as the sarcolemma of the cell acts as a capacitor and is characterized by a difference in voltage across its two faces known as the transmembrane potential (V_m).

The driving force behind the change in transmembrane potential that takes place during an AP is the flow of ions down their concentration gradient, across the membrane through specialized, voltage-gated, membrane-spanning molecules known as ion channels. Ions also flow freely between

neighboring cells through intercellular channels called gap junctions, thus allowing APs to propagate from one cell to the next.

There are two types of APs observed in the heart: slow responses characteristic of the nodal cells, and fast responses observed in the atrial and ventricular myocytes, as shown in Figure 1.2. The fast responses consist of five distinct phases. The initial one, also known as the resting phase or phase 4 is characterized by a transmembrane voltage of about -80 mV caused by the inward rectifier K^+ current (I_{K1}) flowing through the only open channels. Phase 0 starts as an external stimulus brings V_m above the threshold potential of near -40 mV, which in turn causes the I_{K1} channels to close and the Na^+ channels to open (Figure 1.2), allowing Na^+ ions to flow inside the cell and drive the membrane potential up towards the Nernst potential of Na^+. The Na^+ ion channels inactivate rapidly, signaling the beginning of phase 1 in which transient outward K^+ channels activate, allowing K^+ ions to flow outward and the membrane to briefly repolarize (the notch in the AP morphology). Next, the transient K^+ channels close, and the LTCCs and delayed rectifier K^+ channels open, allowing the inward Ca2+ current to balance the outward K^+ current and bringing about the plateau phase (phase 2) of the AP in which the change in the transmembrane potential is minimal. Because LTCC channels deactivate before the delayed rectifier K^+ channels, the delayed rectifier K^+ current (I_K) brings V_m down during phase 3. As I_K channels close and I_{K1} channels open once again, the cell returns to the resting phase.

Although similar, the AP in ventricular cells has a faster upstroke, and longer plateau phase than that in atrial cells, displaying more of a spike-and-dome shape as opposed to a triangular one as seen in the atrial myocytes.

The span of time between phase 0 and phase 3 is called the action potential duration (APD), it can be measured for different levels of repolarization (50% and 90% in Figure 1.2), and is highly variable.

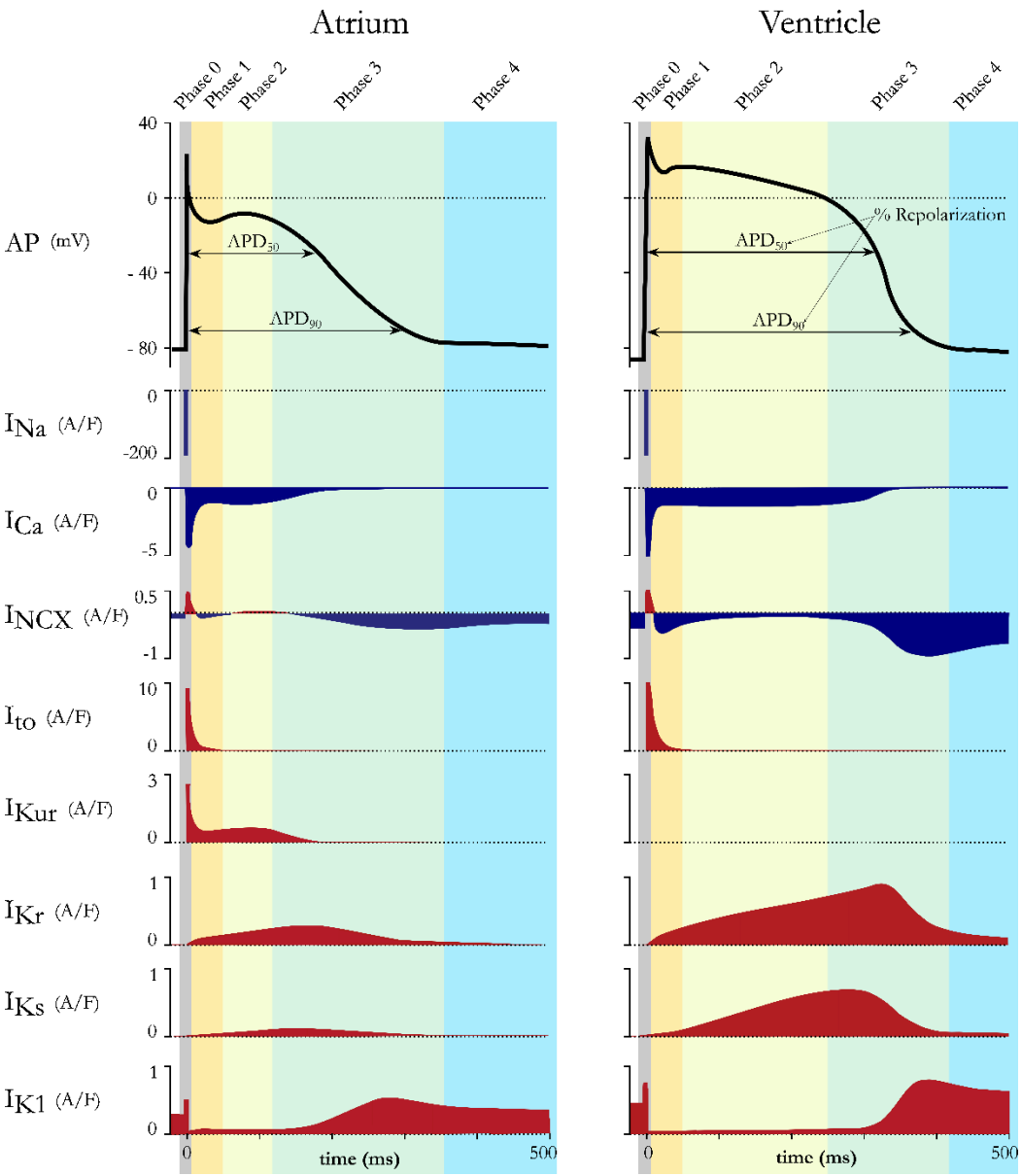

Figure 1.2 Cardiac AP and underlying currents.[1]

[1] Modified from Nerbonne JM. Voltage-regulated potassium channels. In: Zipes D, Jalife J, eds. Cardiac Electrophysiology. 6th ed. Elsevier; 2014.

1.1.2 Excitation-contraction Coupling

Every AP experienced by a cardiomyocyte causes it to shorten in a process known as excitation-contraction coupling. The duration of the action potential in the heart coincides with the duration of the contraction. The main link between the two processes is represented by the increase in the concentration of Ca^{2+} ions inside the cytoplasm during an AP which could not take place without the existence of T-tubules. T-tubules are specialized regions of the sarcolemma which penetrate deep inside the cytosol and carry the electrical signal towards the center of the myocyte (figure 1.3). The sarcoplasmic reticulum (SR) is located in close proximity to these structures and acts as a Ca^{2+} storage unit. A specific molecule called calsequestrin binds to the calcium (Ca^{2+}) ions inside the SR and it allows it to accumulate at very high concentrations. The narrow region between T-tubules and the SR is called the dyadic space. When a stimulus causes the membrane to depolarize during an AP, the voltage-gated LTCCs activate and allow Ca^{2+} ions to flow from the extracellular space, down the concentration gradient, into the dyadic space. There, Ca^{2+} binds to specialized molecules called Ryanodine receptors (RyRs), causing them to open and release a significant amount of Ca^{2+} into the dyadic space – a process called Ca^{2+} - induced Ca^{2+} release (CICR). The high concentration of Ca^{2+} ions inside the dyadic space causes the Ca^{2+}-sensitive LTCCs to close. Ca^{2+} then spreads into the bulk of the cytoplasm. There, Ca^{2+} binds to Troponin C which inhibits Troponin I and leads to a conformational change in Tropomyosin. As this takes place, the binding sites between the actin and myosin filaments become exposed and myosin heads bind do the actin filaments causing cross-bridge cycling and allowing the two filaments to slide against each-other, contracting the whole cell. As cross-bridge cycling ends, Ca^{2+} detaches from the myofilaments and it

is pumped back into the SR by the SERCA pump. At the same time, the Na^{+}/Ca^{2+} exchanger (NCX) and,to a lesser degree, the sarcolemmal Ca^{2+} ATP-ase extrude Ca^{2+} ions from the cell.

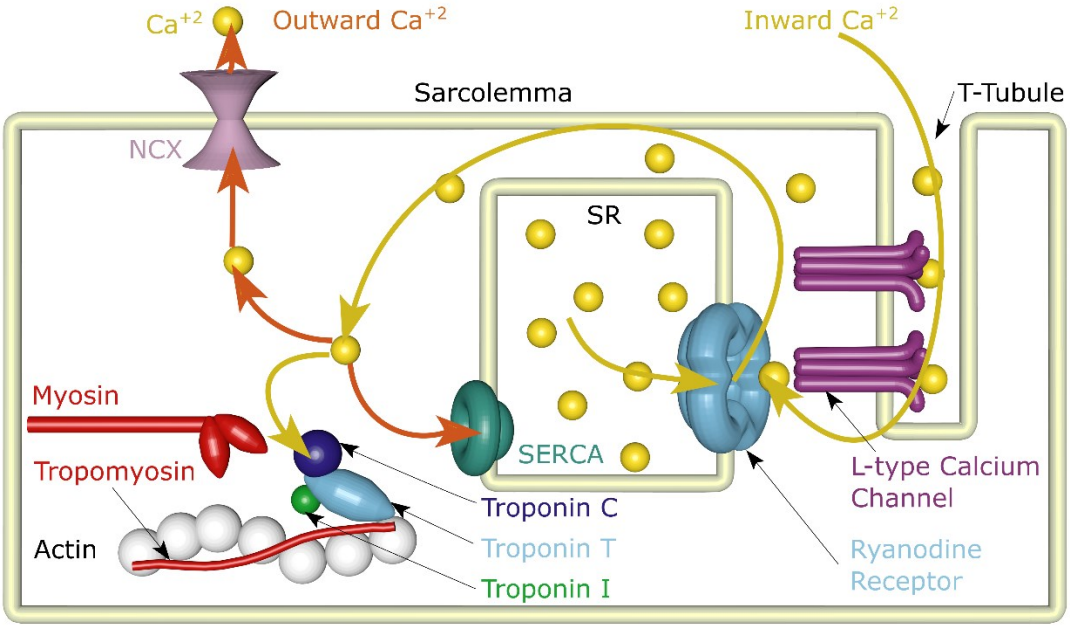

Figure 1.3 Excitation-contraction coupling

1.1.3 Modulation of Cardiac Excitation

Each heart beat originates from the pacemaker cells located in the SA node. Without any external influence, the heart would contract about 100 times each minute. However, the heart rate and cardiac output need to fluctuate in order to meet the body's cells requirements for oxygen and nutrients under varying conditions. Thus, heart rate and contractility (the ability of the cardiac muscle to produce force during a contraction) are regulated by both the sympathetic and the parasympathetic autonomic nervous systems, which have antagonistic effects on the heart. The

human heart is under constant influence of the parasympathetic system via the vagus nerve which causes our resting heart rate to stay around 60-70 beats/min. Sympathetic modulation has the opposite effect, speeding up the heart rate by affecting the slope of Phase 4 of the pacemaker cells in the SA node. In the heart, the main receptors for the catecholamines released by the neurons from the sympathetic nervous systems are the β1 and β2 adrenergic receptors (β1ARs and β2ARs in Figure 1.4). The β1ARs outnumber the β2ARs in cardiomyocytes in a ratio of 4:1. Stimulation of these receptors results in a positive chronotropic effect (increase in heart rate), a positive ionotropic effect (increase in contractility) and a positive dromotropic effect (increase in conductivity). Sympathetic neurotransmitters called catecholamines released by neurons bind to βARs, inducing a conformational change and causing coupling with heterotrimeric G-proteins. G-proteins then dissociate into active Gα and Gβ subunits. Gα subunits proceed to bind to adenylyl cyclase (AC), activating it, and leading to an increase in the production of the second messenger cyclic adenosine monophosphate (cAMP). This messenger molecule is responsible for the activation of numerous other pathways, enzymes, ion channels and transcription factors. For the purpose of this study, the most important enzyme activated by cAMP is the cAMP-dependent protein kinase A which is responsible for the phosphorylation of multiple different substrates within cardiomyocytes.

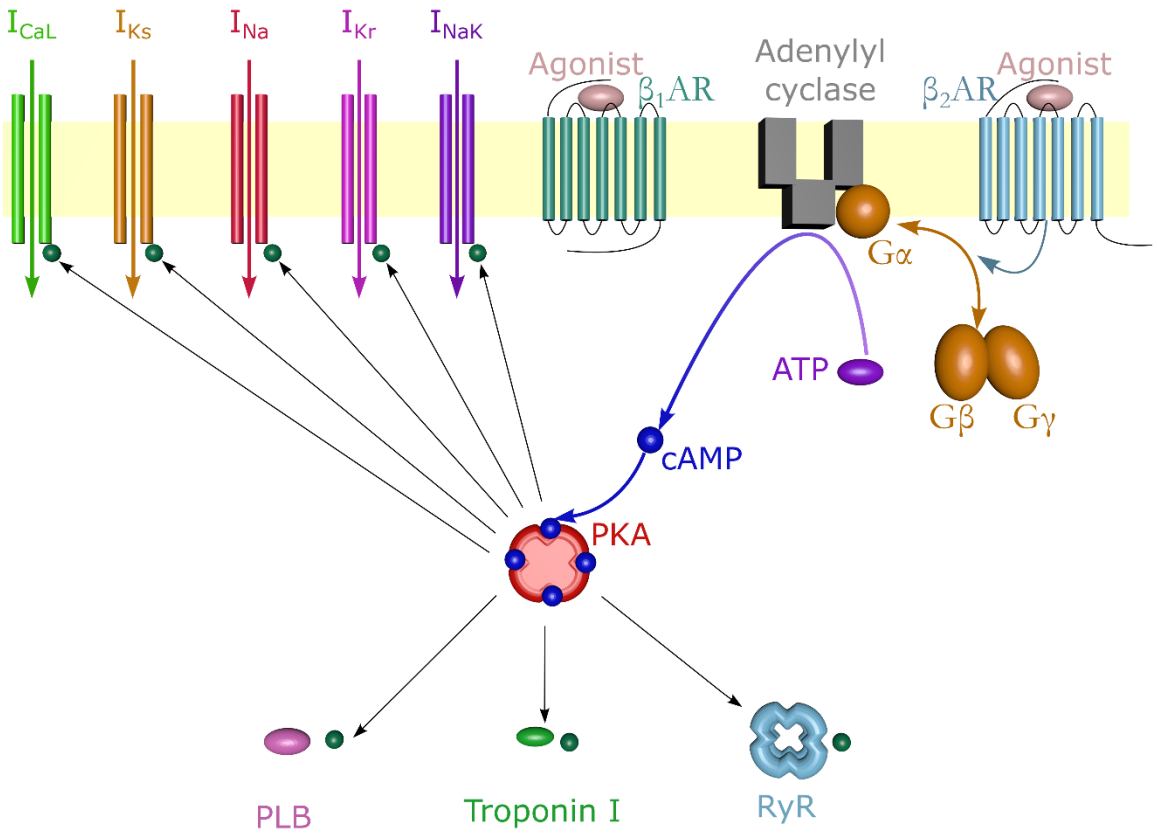

Figure 1.4 Modulation of Cardiac Excitation

1.2 Heart Failure

HF does not have a generally accepted definition. It is described as a syndrome, which develops as a result of an underlying cardiac disease and is recognized clinically based on the many symptoms (e. g. breathlessness, ankle swelling, and fatigue) and signs (e.g. elevated jugular venous pressure, pulmonary crackles, and displaced apex beat) produced by intricate circulatory and neurohormonal responses to altered cardiac function [1], [2]. It is broadly characterized as the pathophysiologic state in which a dysfunction of the cardiac muscle is responsible for the heart failing to pump blood at a rate proportionate to the metabolizing tissues' requirements. HF is one of the most common causes of morbidity and mortality worldwide, constituting a major public health

concern due to the high cost of long-term drug treatment as well as frequent hospitalizations. This economic impact on health services is projected to increase, as the occurrence of HF, currently affecting about 5.7 million Americans is expected to rise by 46% from 2012 to 2030 as the population ages [3]. HF patients are 6 to 9 times more likely to die from sudden cardiac death due to lethal arrhythmias than healthy individuals [4]. Despite these troubling statistics, the mechanism linking pathophysiological remodeling to arrhythmogenesis in HF patients remains poorly understood. This has resulted in ineffective pharmacological therapy for preventing sudden arrhythmic death and in unsuccessful approaches to arrhythmia risk stratification of HF patients [5], [6].

1.2.1 Heart Failure Remodeling

A group of both structural and functional pathological remodeling changes are constantly observed in HF patients [7]. These alterations are detected at various levels of structural organization (molecular, cellular and whole-organ levels), and give rise to ventricular dysfunction and the emergence of malignant arrhythmias. The clinical diagnosis of cardiac remodeling is usually based on detection of structural changes at organ level such as changes in the diameter of the ventricles, mass (hypertrophy or atrophy), the presence of areas of scar after myocardial infarction, fibrosis or inflammatory infiltrates [7]. However, experimental studies have shown that these changes are complemented at cellular and molecular levels by even more remodeling, specifically in the structural and electrophysiological properties of cardiomyocytes, which can trigger the occurrence of ventricular arrhythmias. Looking at transmembrane currents in HF myocytes, we can make a few generalized observations based on available data. The peak of the fast sodium current (I_{Na}) activated

during the depolarization phase of an AP is decreased in HF, while the density of the late sodium current (I_{NaL}) active during the plateau and repolarization phases is increased. The LTCC current density remains the same, while all potassium currents (I_{to}, I_{K1}, I_{Kr} and I_{Ks}) show a decrease. Lastly, the activity of the SERCA and NaK pumps in HF is downregulated, while that of the NCX is upregulated [8]. All these changes, combined with a disruption of the T-tubular microdomain have been sowed to give rise to triggers of arrhythmia such as early and delayed afterdepolarizations (EADs and DADs).

1.3 Objectives

The goal of this work was to explore a novel set of mechanisms by which HF remodeling, specifically at subcellular domain leads to an increased risked of lethal arrhythmias in human HF. The specific aims of this work were:

• Specific Aim 1: Identify the cellular mechanisms by which degradation of subcellular microdomains in HF myocytes impact the function of LTCC and lead to the generation of cellular-level triggers of arrhythmia.

• Specific Aim 2: Evaluate the difference between the nanoscale regulation of L-type Calcium channels in ischemic vs dilated cardiomyopathies and how these impact arrhythmogenicity.

Chapter 2: General Methods

2.4 Cardiac Computational Modeling

The electrophysiological functions of the heart described above can be simulated with high accuracy using mathematical modeling. Features from molecular, cell, and tissue levels can be integrated using computer simulations in order to study their contributions to both normal cardiac function as well as organ-scale arrhythmogenic phenomena. Product of decades of research, modern-day models of atria and ventricles allow scientists to study cardiac electrophysiology at a high spatiotemporal resolution, and propose solutions to current clinical problems. The building blocks of such models and the methods used in cardiac computational modeling are described in the sections below.

2.5 Hodgkin and Huxley vs. Markov Formalism

The first mathematical model able to reproduce transmembrane currents and APs was formulated by Hodgkin and Huxley in 1952, based on their observations of the squid giant axon's electrophysiology. In their model, an ion channel can be either open or closed, depending on the states of the channel's gates. As the behavior of each gate is assumed to be independent from that of the other gates of the channel, the current through such a channel is a time- and voltage-dependent function directly proportional to the open probabilities of the channels' gates. The ionic current thus defined, along with a capacitive current sum up to give the total membrane current:

$$I_m = C_m \frac{dV_m}{dt} + I_{ionic} + I_{stim}$$

Im represents the total membrane current density, Cm is the membrane capacitance per unit area, Vm represents the transmembrane potential, Iionic is the total ionic current density, and Istim represents the current density of a transmembrane stimulus. Many modern computational AP models (Grandi et al., 2010; Luo and Rudy, 1994; O'Hara et al., 2011; ten Tusscher et al., 2004) use the Hodgkin and Huxley formalism to describe membrane kinetics. By subdividing I_{ionic} into multiple components such as I_{Na}, I_{NaL}, I_{CaL}, I_{K1}, I_{to}, I_{Kr}, I_{Ks}, I_{NaCa}, and I_{NaK} based on detailed experimental measurements using voltage clamping, and numerically integrating these equations, scientists have been able to successfully reproduce APs from various cell types within the hearts of different species. An equivalent formalism to that of Hodgkin and Huxley, but based on Markov chains can be used to substitute the equations for one or all ionic currents. In this paradigm, Markov chains are used to represent the time- and voltage- dependent state transitions for each individual ion channel. The ionic current can, in this case, be expressed as a function of the occupation of the open state. Markov formalism is usually used to represent the behavior of ionic currents when genetic mutations are present, but can also successfully model wild-type ionic currents. Although for the purpose of this study we can represent our ionic currents using either formalism, computing the ionic currents using the Markov method usually requires a larger number of state variables and more computational power. This has a small effect in single-cell simulations, but can lead to a considerable increase in computational time in whole-organ 3D simulations. Therefore, while we will use Markov formalism to calibrate our models in the second part of this work, in our whole organ simulations we will use the Hodgkin and Huxley formalism exclusively.

Chapter 3: Degradation of T-Tubular Microdomains and Altered cAMP Compartmentation Lead to Emergence of Arrhythmogenic Triggers in Heart Failure Myocytes: An In-Silico Study

This study has been published in Frontiers in Physiology [9].

3.1 Introduction

HF causes the heart to undergo remodeling across multiple scales [10]. However, studies have shown that nearly all arrhythmias in non-ischemic heart failure and approximately 50% of those in ischemic heart failure develop due to abnormal automaticity or triggered activity such as EADs and DADs [11].

Previous research has also shown that remodeling at cellular and subcellular levels characteristic of HF can lead to AP prolongation and delayed repolarization, which could be important causes of EAD formation. In turn, these changes could be linked to the modification in ion channel behavior, especially the LTCC whose activity is highly regulated via cAMP by various molecules co-localized in the T-tubular region, and the disruption of intracellular Ca^{2+} handling also

observed in unhealthy myocytes [10], [12], [13]. These subcellular changes are often exacerbated by sympathetic stimulation which increases the levels of cAMP and can cause an increase in inward current, particularly through LTCCs. This, in turn, can destabilize the labile plateau phase of APs [4]. However, the exact mechanism linking changes in T-tubule organization and in cAMP compartmentation to abnormal LTCC function and the development of arrhythmogenic triggers remains unknown.

LTCCs play an important role in excitation-contraction coupling and influence the electrical and mechanical functioning of cardiac muscle [14]. In ventricular myocytes, under normal conditions, LTCCs are clustered in the transverse tubules (T-tubules). Gradual T-tubule loss, a known effect of HF, forces LTCCs to be redistributed to the surface membrane where they maintain their function but experience a different environment than that of the dyadic space [15].

Within the T-tubules, LTCCs are usually associated with a number of specific macromolecular signaling complexes and scaffolding proteins which allow for precise control of Ca^{2+} signaling [16], [17]. One such signaling complex is the β_2AR, responsible for mediating the functional effects of cathecolamines in the heart, and more specifically, inside T-tubules, where they are confined. Selective sympathetic stimulation of the two receptor subtypes, β_1AR and β_2AR, lead to distinct physiological responses, based on their different localization and kinetics [18]. β_1ARs stimulate the cAMP-dependent PKA-mediated phosphorylation of phospholamban and cardiac contractile proteins. Sympathetic stimulation of the β_2AR, on the other hand, activates the G-protein/adenylyl cyclase (AC)/cAMP/PKA pathway which leads to the phosphorylation of several substrates, including LTCCs. In failing cardiomyocytes β_2ARs are redistributed from the T-tubular

membrane to the non-T-tubular membrane areas where stimulation of the receptor induces far reaching cAMP signals, similar to those elicited by β_1AR stimulation [19], [18].

Apart from the molecules mentioned above, PDEs, which cleave cAMP into adenosine monophosphate (AMP) and protein phosphatases that dephosphorylate LTCCs also have an effect on the phosphorylation state of LTCCs. Furthermore, PDE molecules also show a high localization to the T-tubule membrane in healthy cells and along with AC and PKA play a key role in controlling the compartmentation of cAMP (Heijman, Volders, Westra, & Rudy, 2011). Activation of PKA by cAMP leads to PDE phosphorylation, increasing its activity, which in turn removes phosphorylation from other molecules. Thus, PDEs provide a negative feedback-loop for cAMP level control. Disrupting the localized PDE expression could lead to increased levels of cellular cAMP and inhibition of the PDE hydrolyzing effect [19].

The goal of this study was to uncover the mechanism by which HF-induced changes in cAMP compartmentation combines with the LTCCs T-tubule-to-surface-membrane redistribution to cause an abnormal LTCC current which promotes the development of EADs in human ventricular myocytes. To this end, we developed a novel model, using the O'Hara-Rudy human cardiac ventricular AP formulation [21] combined with the Heijman et al. β-adrenergic signaling simulations [22] as our cornerstone. As the specific aim of this study was to dissect the effects of β_2AR signaling localization loss and PDE-dependent cAMP level control impairment on the electrophysiological function of the cell, our single-cell model brought together various aspects of microdomain remodeling characteristic to HF, such as LTCC redistribution presented by Sanchez and colleagues [15], and modified cAMP compartmentation observed experimentally by Nikolaev

and colleagues [18]. Our results show valuable insight into the pathophysiological changes that favor the development of cellular arrhythmogenic triggers in HF patients.

3.2 Methods

3.2.1 Overview of the Modeling Approach to Simulate the Behavior of Human HF Ventricular Myocyte

As a baseline model representing the healthy human ventricular myocyte, we used the O'Hara-Rudy human ventricular AP model [21] combined with the Heijman et al. β-adrenergic signaling model [22], as described previously [8]. Within this model, the behavior of the LTCCs is described using a Hodgkin-Huxley formulation, and LTCC CDI depends on the concentration of Ca^{2+} the channels sense. To simulate a human HF ventricular myocyte, we incorporated various changes into the baseline model, reproducing ionic and structural remodeling observed in vitro, and described in detail in the sections below.

First, similar to a previous study [15], we introduced T-tubular microdomain loss, resulting in LTCCs and Na^{+}/Ca^{2+} exchangers (NCXs) being redistributed from the T-tubular membrane to the bulk of the sarcolemma and in RyRs decoupling from LTCCs. However, instead of creating a single model of an HF ventricular myocyte as in the study by Sanchez and colleagues, we permitted the amount of microdomain loss to vary and thus created a family of HF myocyte models that allowed us to analyze different stages of the disease. The progression of the disease was also modeled by letting the phosphorylation level of the channels to vary based on the presence of β_2ARs and PDEs in both the T-tubular space and in the bulk of the cytoplasm or sarcolemma. The more advanced the

stage of the disease was, the more PDE molecules were redistributed from the dyadic space to the bulk of the cytoplasm, and the more β_2ARs were shifted from the T-tubular to the surface membrane. Since LTCCs would display a different behavior based on their location and the signaling domain they experience, we divided LTCCs within a myocyte into 6 different subgroups (Subgroups A – F) based on their position in the T-tubular or surface membrane and their signaling environment, where they may or may not experience the phosphorylating effect of PKA and the hydrolyzing effect of PDEs (Figures 3.1A – 3.1F). The resulting models containing all LTCC populations were utilized to carry out computer simulations uncovering the mechanisms responsible for the generation of EADs in human HF myocytes under adrenergic stimulation.

3.2.2 Introducing T-tubular Microdomain Degradation in HF

The combined O'Hara-Rudy and Heijman model contained LTCCs exclusively in the T-tubular membrane[23]. We used a similar approach to that in the study by Sanchez and colleagues [15], and allowed for LTCCs to be redistributed to the surface membrane. Thus, in addition to the already defined dyadic volume, we included a sub-sarcolemmal volume which allowed for Ca^{2+} accumulation near the intracellular mouth of LTCCs in the surface membrane. We described fluxes from and into this volume in the O'Hara-Rudy myocyte model [21] based on the work of Grandi and colleagues [24] and Shannon and colleagues [25]. Similar to Sanchez et. al., we modeled the relocation of LTCCs to the surface membrane by allowing the redistributed channels to contribute to and sense the Ca^{2+} concentration from the sub-sarcolemmal volume as opposed to the dyadic volume for those remaining in the T-tubular membrane. However, to study the progression of the disease, we created multiple models in which T-tubule microdomains were gradually lost. In order to

account for this HF-induced T-tubular degradation, we introduced the parameter f_TT in the model and used it to encode T-tubule integrity. The value of this parameter was allowed to range from fully intact (f_TT=1.0, 0% t-tubule loss) to completely degraded (f_TT=0.0, 100% T-tubule loss) in increments of 0.1. We then set the fraction of LTCCs that were redistributed from the T-tubule to the surface membrane to be directly proportional to the loss of T-tubules. Thus, when the T-tubular membrane was intact (f_TT=1.0), all LTCCs were confined to it. In contrast, when the microdomain was completely disrupted (f_TT=0.0), all LTCCs were redistributed to the surface membrane.

3.2.3 Modeling the Effect of T-tubular Loss on the Na^+/Ca^{2+} Exchanger and RyRs

Two other molecules affected by the loss of T-tubular domains are the NCX molecules and RyRs. In the original O'Hara-Rudy model, RyRs are always associated with LTCCs from the T-tubular membrane and only a fifth of the NCX are located in the surface membrane, while the rest reside in the T-tubular subspace [21]. The choice of including 20% of NCX molecules in the bulk of the sarcolemma is consistent with previous models [26], [27] and was validated based on its effect on the rate dependence of peak $[Ca^{2+}]_i$ in [28]. We used the same approach as in the study by Sanchez and colleagues, and redistributed a fraction of NCXs proportional to the amount of de-tubulation from the T-tubular sites to the sarcolemma based on observations made by Gadeberg and colleagues[29]. The same fraction, but this time of RyRs, was also decoupled from LTCCs [15].

3.2.4 Representing the Effect of β_2ARs and PDEs Presence on LTCCs

Activation of the β_2AR leads to an increase in adenylyl cyclase (AC) activity which, in turn, increases the levels of cAMP. Next, cAMP binds to the regulatory subunits of PKA, enabling the catalytic subunits to phosphorylate their substrates at specific serine or threonine residues. This signaling cascade is counterbalanced by the hydrolyzing activity of PDEs. Specifically PDE3, and to a lesser extent PDE4 predominantly determine cAMP levels in the cytosol as well as in the dyadic space, by degrading cAMP [22]. While there are more isoforms of PDE [30] and models developed for each of them, we chose to focus exclusively on PDE3, as drugs that restore PDE3 activity in ischemic and dilated cardiomyopathies have been shown to have a cardio-protective effect. Because there is only one detectable phosphorylation site that allows PKA to regulate LTCCs [31], an LTCC can be characterized by one of two conditions: phosphorylated or not phosphorylated. In other words, an LTCC cannot be partially phosphorylated, and phosphorylation can be modeled as a binary process. Based on these observations, we divided all LTCCs within a myocyte into two different populations, phosphorylated and not phosphorylated. Thus, in order to simplify our model, we only used the electrophysiological module of the Heijman et al. β-adrenergic signaling model [22], we fixed the phosphorylation levels for the base model, so that it matched experimental measurements, and modeled PDE activity loss to be directly proportional to the T-tubular microdomain loss.

Therefore, we also introduced two new parameters, f_PDE and f_B2AR to quantify the fractions of LTCCs that experience phosphorylation due to the activation of the β_2AR /G-protein/AC/cAMP/PKA signaling cascade and dephosphorylation due to PDE activity. In other

words, localized upregulation of I_{CaL} due to β_2AR stimulation was encoded to affect only a certain proportion of LTCCs, which varied from all LTCCs (f_B2AR = 1.0) to none (f_B2AR =0.0) in increments of 0.1. Similarly, the hydrolyzing activity of PDEs was allowed to range from affecting no LTCC (f_PDE = 0.0), to affecting all LTCCs (f_PDE = 1.0) in steps of 0.1.

3.2.5 Allowing LTCCs to Function in Different Locations and Signaling Domains

A comprehensive population-based approach in which LTCCs were distributed between the 6 different subgroups mentioned in the overview and described below was then used to integrate the effects of T-tubule loss and the disruption of β_2AR and PDE signaling localization on the LTCC current in HF myocytes. The Hodgkin-Huxley formulation of LTCC current combines together the number of LTCCs and their conductance in order to obtain a current density for the whole cell. Empirically, no significant changes in LTCC current density have been observed in failing human cardiac myocytes [32], [33], which may be due to heart failure myocytes showing a decrease in LTCC number, paired with an increase of the channel's activity [34]. However, in our myocyte model the total number of LTCCs and their conductance were kept constant, each LTCC being assigned a current (I_{CaL}) equal to unity. This assumption was made in order to limit the degrees of freedom of our model, to be able to draw mechanistic insights from the data obtained. If an LTCC was phosphorylated by PKA, the amplitude of the current through that channel was increased by a factor of 2.5 [22]. Subgroup A, depicted in Figure 3.1, Subgroup A, contains channels identical to the LTCCs found in healthy myocytes: they are located in the T-tubular membrane and experience

cAMP levels regulated by both PKA and PDE. In the second group – subgroup B (Figure 3.1, Subgroup B), LTCCs located in the T-tubular membrane do not experience the hydrolyzing activity of PDE, so they are assumed to always be phosphorylated. In contrast, the subgroup C of LTCCs (Figure 3.1, Subgroup C), which experience the activity of PDE, are assumed to never be phosphorylated as they lack association with β_2ARs. Based on this logic, another subgroup could be defined as the channels lacking both PDE and β_2AR in the T-tubular membrane, but physiologically, these would be indistinguishable from the channels in Subgroups C as they would never be phosphorylated. Therefore, we assumed they are also part of Subgroup C. The other three groups (Subgroups D - F) are similar to the ones just mentioned but are located in the surface cellular membrane as opposed to the T-tubular membrane. The total LTCC current for a cell was calculated as the sum of the currents passing through each channel population.

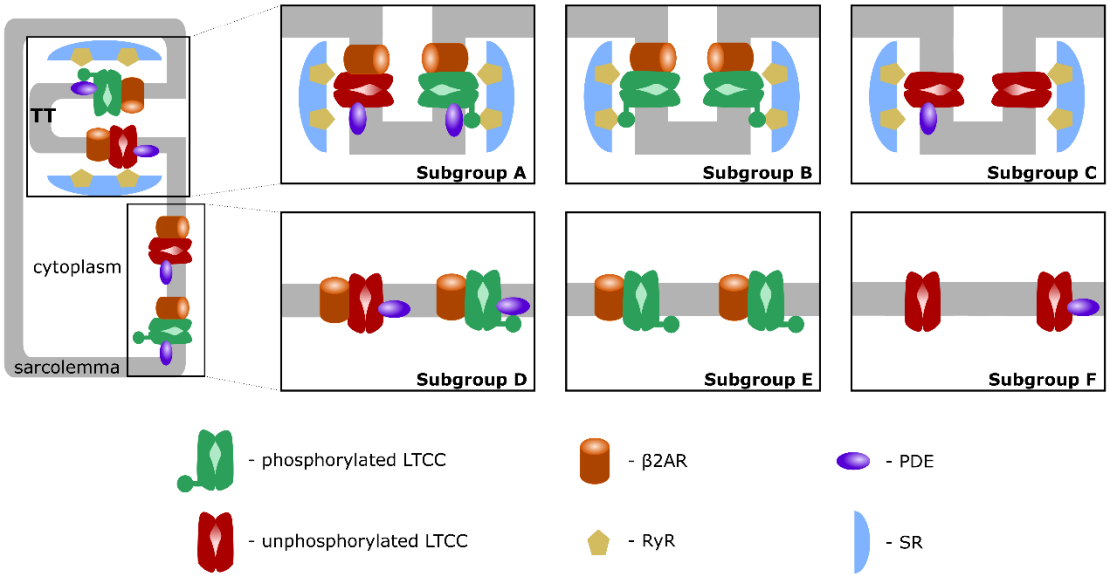

Figure 3.1 Schematic representation of LTCC subgroups A-F. LTCCs are located either in the T-tubular membrane (Subgroups A, B, C) or in the bulk of the sarcolemma (Subgroups D, E, F). LTCCs were either associated with both β_2ARs and PDEs (Subgroups A, D), solely with β_2ARs (Subgroups B, E), or not associated with β_2ARs at all (Subgroups C, F). The channels were either phosphorylated (red) or unphosphorylated (green).

3.2.6 The Effects of Phosphorylation on Other Molecules

A similar population-based approach was used to represent the degree of PKA phosphorylation, in the presence or absence of β_2AR stimulation, of seven different targets: RyR, Phospholamban (PLB), Slow Delayed Rectifier K^+ Current (I_{Ks}), Fast Na^+ Current, Na^+/K^+ATP-ase Current (I_{NaK}), rapidly activating K^+ current (I_{Kur}) and Troponin I (TnI), as described by Heijman and colleagues [22].

Assuming that channel gating has no effect on phosphorylation, the molecules mentioned above can have only two distinct conformations (phosphorylated and non-phosphorylated). Therefore, each of the seven phosphorylation targets were divided into two subgroups: phosphorylated and not phosphorylated. The effect of phosphorylation on each target, as described by Heijman and colleagues [22], was included in the model. Basal conditions were modeled to account for the phosphorylation of 25% of targets while β_2AR stimulation led to the phosphorylation of 75% of each substrate population. These values were chosen in order to obtain LTCC current traces in the healthy myocytes similar to those experimentally recorded and presented by Bryant and colleagues [34]. In order to be as physiologically accurate as possible, the model also accounted for CaMKII-dependent phosphorylation of I_{CaL}, I_{Na} and late I_{Na} ($I_{Na,L}$) based on recently

published data [15]. For each of these molecules it was assumed that PKA and CaMKII phosphorylation are independent processes. Therefore, the targets were divided into four populations. At each time step, the currents through the LTCCs and I_{Na} channels were computed for both (phosphorylated and non-phosphorylated) populations. The total current was obtained by adding together the currents through each population and thus integrating the β_2AR and CaMKII cascades. While the level of PKA phosphorylation varied for the purpose of this study, the CaMKII phosphorylation level was kept constant.

3.2.7 I_{CaL} and Action Potential Duration (APD) Analysis Protocol

APD_{90} was computed as the time point of 90% repolarization of the membrane potential minus the time point of maximal upstroke velocity $(dV/dt)_{max}$. For the first part of the study, we established 6 different cases (case 1- 6) in which 80% of LTCCs within a cell were assigned to one of each of the six subgroups described above and in Figure 3.1, and for each case the remaining channels were distributed between the other 5 subgroups (Figure 3.2). This allowed us to observe and analyze separately the effects of LTCC redistribution, loss of β_2AR signaling localization, and PDE's impaired control of cAMP on the LTCC current and APD_{90}. The model myocyte was first allowed to reach steady state under a voltage clamp of -96.7 mV. To determine the effect of each parameter (f_TT, f_B2AR and f_PDE) on the LTCC current, the membrane voltage was then stepped up from -96.7 mV to -6.7 mV, clamped again, and the LTCC current was recorded. In order to analyze the effect of the same parameters on APD_{90}, the myocyte was paced at near resting pacing rates (1000 ms, 60b pm) until steady state was reached; the following 3 beats were recorded.

3.2.8 Protocol for Evaluating EADs in the Human Ventricular AP Model

The same protocol used to analyze APD_{90}, was also used to investigate how the model variables drive the emergence of EADs. The myocyte was again paced at near resting pacing rates (1000 ms, 60 bpm) for 1000 cycles and the following 15 beats were recorded. For this part of the study, LTCCs were distributed into the 6 different subgroups represented in Figure 3.1 by varying the model variables f_TT, f_B2AR and f_PDE. The probability that an LTCC was corresponding to one of the subgroups was computed by multiplying these state variables. The procedure was repeated for values of f_TT and f_PDE uniformly covering the range of possible values from 0.0 to 1.0 in increments of 0.1, and for values of the f_B2AR ranging from 0.0 to 1.0 in increments of 0.25. The APs generated both in the presence and absence of adrenergic stimulation were analyzed.

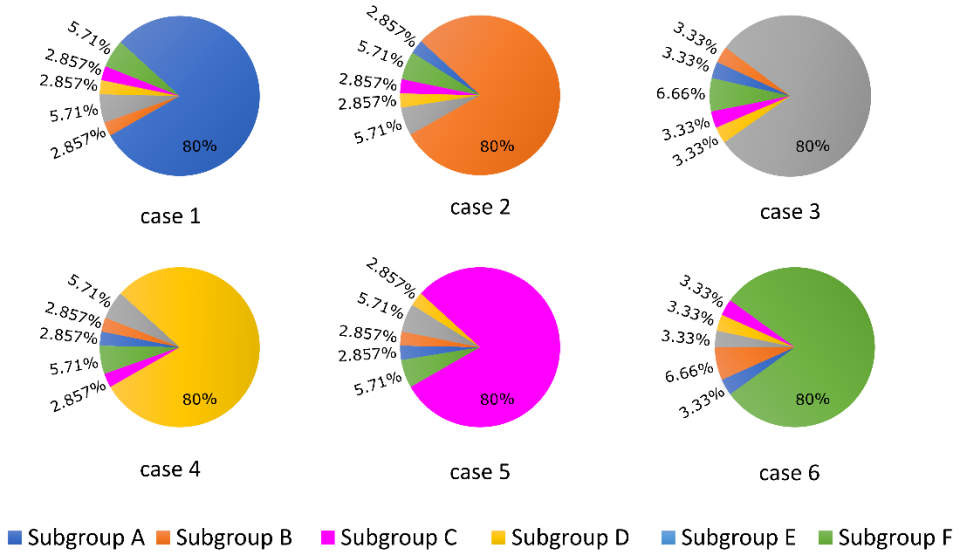

Figure 3.2 LTCC distribution between the 6 different subgroups (A-F) for each case analyzed (1-6). The total number of LTCCs in the cells from each case was kept constant, but the channels were divided into the 6 Subgroups in the ratios displayed. In case 1, 80% of the channels are located inside the T-tubular membrane, while the remaining ones were distributed to the remaining subgroups based on their probability to be associated with PDEs and β_2ARs. In case 2, the dominant channel population was represented by channels located in T-tubules, lacking PDE association, while in case 3, the majority of channels were also located in the T-tubular membrane, but were not associated with β_2ARs. Cases 4, 5 and 6 are similar to Cases 1, 2, and 3, but their dominant channel populations are located in the surface sarcolemma.

3.3 Results

3.3.1 HF Remodeling Leads to a Higher Amplitude, Longer Lasting LTCC current.

The LTCC current traces from the cases outlined in Figure 3.2 are plotted in Figure 3.3 under both basal and adrenergic stimulation conditions. The control case (Figure 3.3, case 1 - black) was represented by the LTCC current in the healthy myocyte with intact tubulation as well as localization of β_2AR and PDE activity. LTCC current decay was rapid, especially in the T-tubules (τ_1=18.7 ms, τ_2=318.3 ms), due to the strong CDI caused by the accumulation of Ca^{2+} in the dyadic volume of the model. β_2AR stimulation in the control case led to an increase in the magnitude of LTCC current and a faster decay rate (τ_1=18.3 ms, τ_2=257 ms), as compared to the basal conditions (Figure 3.3, case 1 - red). The effect of PDE on controlling cAMP levels and thus LTCCs level of phosphorylation was evaluated by removing PDE from the model (Figure 3.3, case 2). Although this change had little to no effect for the case with basal PKA phosphorylation (black), it considerably increased LTCC current peak when adrenergic stimulation was applied (red). This showed that PDE has a protective role that helps lower inward LTCC current, as PKA activity was not inhibited at all

by the hydrolyzing activity of PDE on cAMP. Removing all β_2ARs led to smaller currents as PKA did not phosphorylate any channel (Figure 3.3, case 3). In the control case, when tubulation was removed and LTCCs shifted to the surface membrane (Figure 3.3, case 4), Ca^{2+} was not able to accumulate in significant amounts in the proximity of the LTCCs. Thus CDI was delayed, peak current was elevated, and I_{CaL} inactivation rate was lower (τ_1=29.0 ms, τ_2=3392 ms). Applying β_2AR stimulation in this case led to an even larger in magnitude and slower current (Figure 3.3, case 4 – red), and removing PDE further exacerbated this effect (Figure 3.3, case 5). Removing T-tubules when β_2ARs were absent (Figure 3.3, case 6) led to a slower decaying current, of similar magnitude to that in fully tubulated cells. Overall, subcellular changes associated with the HF phenotype, such as de-tubulation, LTCC redistribution to the surface membrane, and loss of β_2AR and PDE signaling localization, led to an increase of the LTCC peak current and a delay in the channels' inactivation.

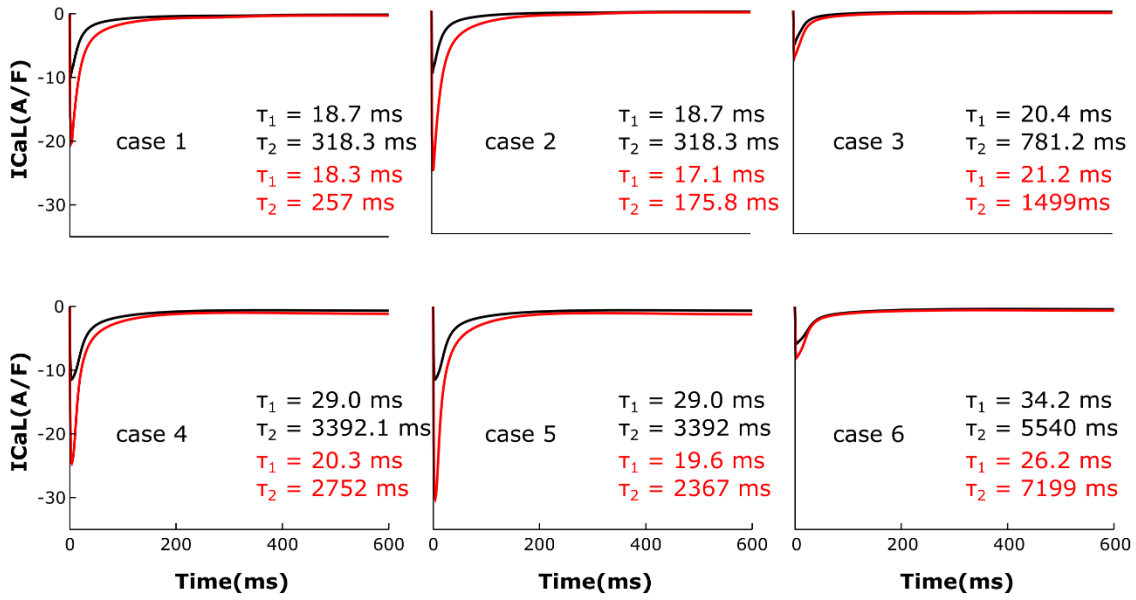

Figure 3.3 The effect of microstructure remodeling on LTCC current. Total LTCC current was plotted over time from cells corresponding to cases 1-6 described in methods, under both basal (black) and sympathetic stimulation (red) conditions. The decay time constants for the current through the channels in the T-tubules and the ones in the bulk of the sarcolemma were displayed as τ_1 and τ_2.

3.3.2 HF Remodeling Leads to Altered SR Ca Release and Ca transient

For each of the cases described above, the Ca^{2+} flux from the SR into the cytoplasm through RyRs is plotted in Figure 3.4 and the Ca^{2+} concentration inside the cytoplasm in Figure 3.5. When adrenergic stimulation is applied, the β_2AR /G-protein/AC/cAMP/PKA signaling cascade is triggered, which leads to the phosphorylation of RyRs along with LTCCs. Thus, not only do RyRs experience a higher Ca^{2+} concentration in the dyadic space due to the phosphorylation of LTCCs, but their activity is also enhanced by direct PKA phosphorylation, leading to a higher Ca^{2+} flux from the SR into the cytoplasm (Figure 3.4). However, due to the higher Ca^{2+} concentration inside the dyadic space, RyRs deactivate faster under adrenergic conditions, and the Ca^{2+} concentration inside the cytoplasm does not differ greatly between baseline and adrenergic stimulation conditions in intact myocytes (Figure 3.5). The β_2AR enhancing effect on Ca^{2+} release appears stronger when the microdomain is degraded. By removing T-tubules, we disrupt the association between LTCCs and RyRs within the dyadic space. Removing T-tubules and relocating LTCCs from the dyadic space to the surface of the membrane leads to a lower Ca^{2+} concentration within the dyadic volume, and a

weaker release of Ca^{2+} from the SR into the cytoplasm. While completely removing β_2AR molecules in the intact HF myocyte model leads to a lower amount of Ca^{2+} being released via RyRs in, it has the opposite effect in de-tubulated cells (Figure 3.4). This is explained by the fact that LTCCs in the surface membrane experience CaMKII phosphorylation, while those in the T-tubular membrane do not [15]. Overall, the Ca^{2+} concentration inside intact myocytes is higher than that in de-tubulated cells due to higher LTCC current through T-tubular channels, and an increase in the flux of Ca from the SR into the cytoplasm.

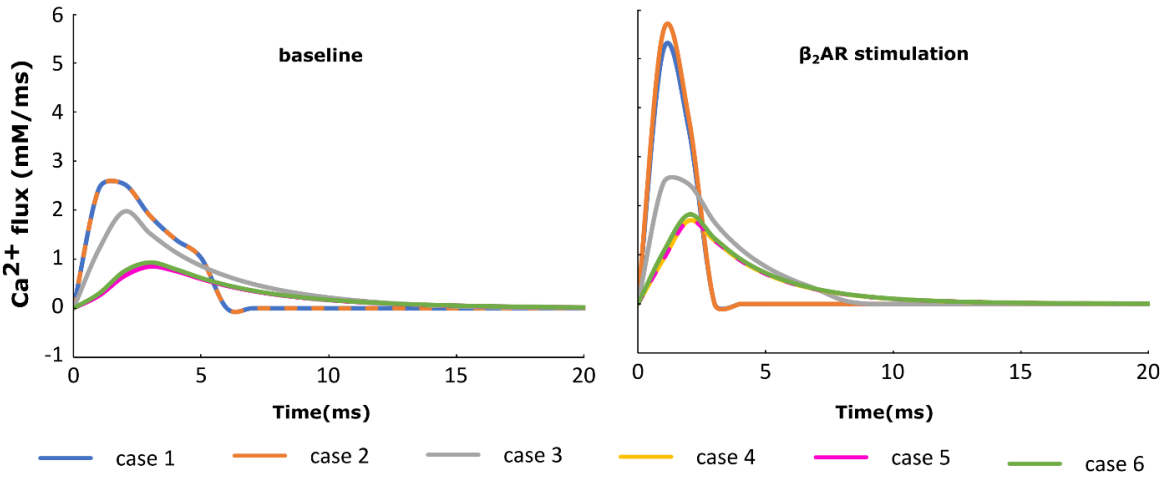

Figure 3.4 The effect of microstructure remodeling on SR Ca^{2+} release.
The Ca^{2+} flux from the SR into the cytoplasm via RyRs was plotted over time from cells corresponding to cases 1-6 , under both basal (left) and sympathetic stimulation (right) conditions.

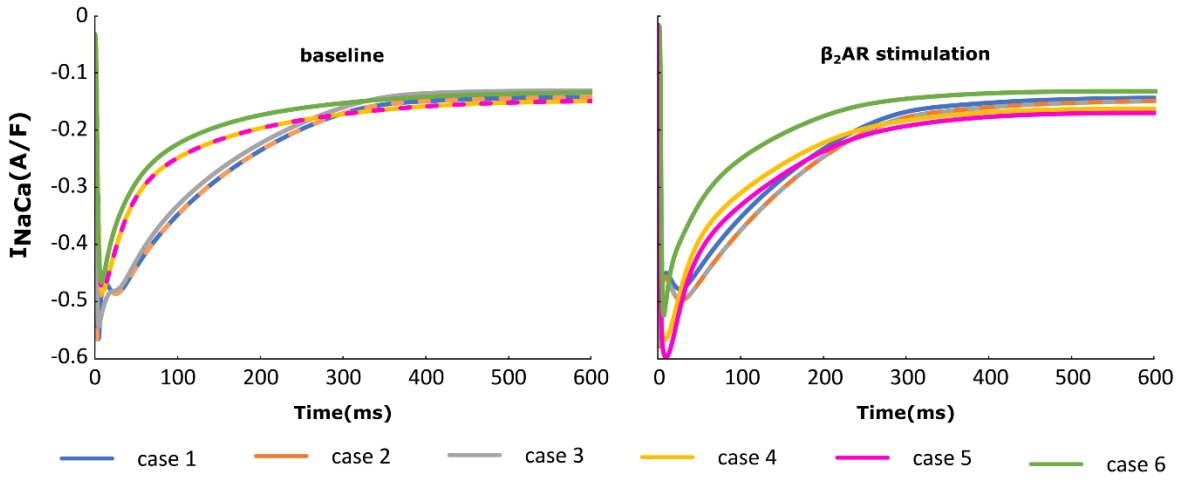

Figure 3.5. The effect of microstructure remodeling on I_{NaCa} current.
The I_{NaCa} current was plotted over time from cells corresponding to cases 1-6, under both basal (left) and sympathetic stimulation (right) conditions.

3.3.3 Changes in I_{CaL} and RyR Function Impact the NCX Current.

The NCX current traces from the cases outlined in Figure 3.2 are plotted in Figure 3.6 under both basal and adrenergic stimulation conditions. Similar to the re-distributed LTCCs, NCX molecules which shifted to the surface membrane experience the Ca^{2+} concentration from the sub-sarcolemmal volume. Under baseline conditions, microdomain loss lead to a small decrease in I_{NaCa} corresponding to a lower SR Ca release and an overall lower Ca^{2+} transient. However, similar to I_{CaL}, under adrenergic stimulation I_{NaCa} displayed an increase in amplitude when the myocyte underwent de-tubulation, but not a slowdown in decay rate. These results can be explained based on the observations we made before on RyR and LTCC function. NCX is an antiport driven by the concentration gradients of Ca^{2+} and Sodium. A high amplitude I_{CaL} within a de-tubulated cell leads to a high concentration of Ca inside the sub-sarcolemmal volume which in turn causes a steep gradient

between the inside and outside of the cell. Thus, we observe a high amplitude I_{NaCa} under adrenergic stimulation in the HF myocyte, which in theory should lead to APD shortening.

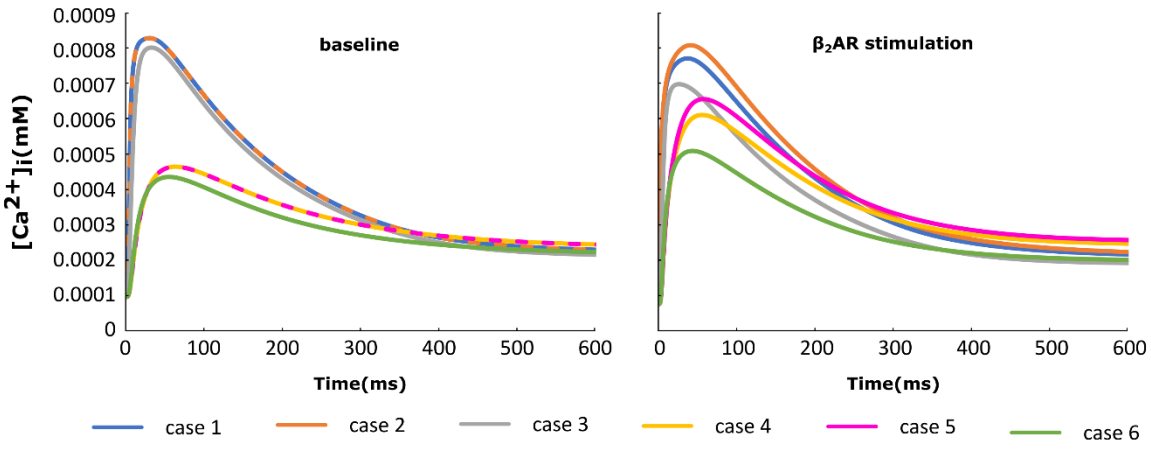

Figure 3.6 The effect of microstructure remodeling on Ca^{2+} transient.
The Ca^{2+} concentration inside the cytoplasm was plotted over time from cells corresponding to cases 1-6 described in methods, under both basal (left) and sympathetic stimulation (right) conditions.

3.3.4 Abnormal LTCC Current Affects APD_{90}

We then analyzed the effect of varying the parameters encoding for T-tubule integrity, β_2AR and PDE on AP shape and duration. The membrane potential corresponding to the six cases described above was plotted in Figure 3.7. For the control case under no adrenergic stimulation, an APD_{90} of 281 ms was recorded. Adding β_2AR stimulation lead to an increase and slower decay rate in the LTCC current, which caused a slight prolongation of APD_{90} to 308 ms (Figure 3.7, case 1). Removing PDEs from the model and applying β_2AR stimulation caused the emergence of single EADs in intact myocytes (Figure 3.7, case 2). Removing all β_2ARs from the model, on the other hand, had the opposite effect, preventing EADs and causing APD_{90} to shorten (Figure 3.7, case 3). When tubulation was removed from the control case, and no adrenergic stimulation applied, the observed increase in LTCC current led to a corresponding 44 ms APD_{90} prolongation.

The effect of β_2-stimulaton was significantly stronger in the absence of T-tubules resulting in an APD_{90} of 517 / 668 ms and the development of multiple EADs (Figure 3.7, case 4). However, in de-tubulated myocytes, applying adrenergic stimulation while lacking PDE led to an oscillatory state in which the cells did not repolarize before the next stimulus was applied (Figure 3.7, case 5). Removing all β_2ARs from the de-tubulated model prevented EAD formation (Figure 3.7, case 6).

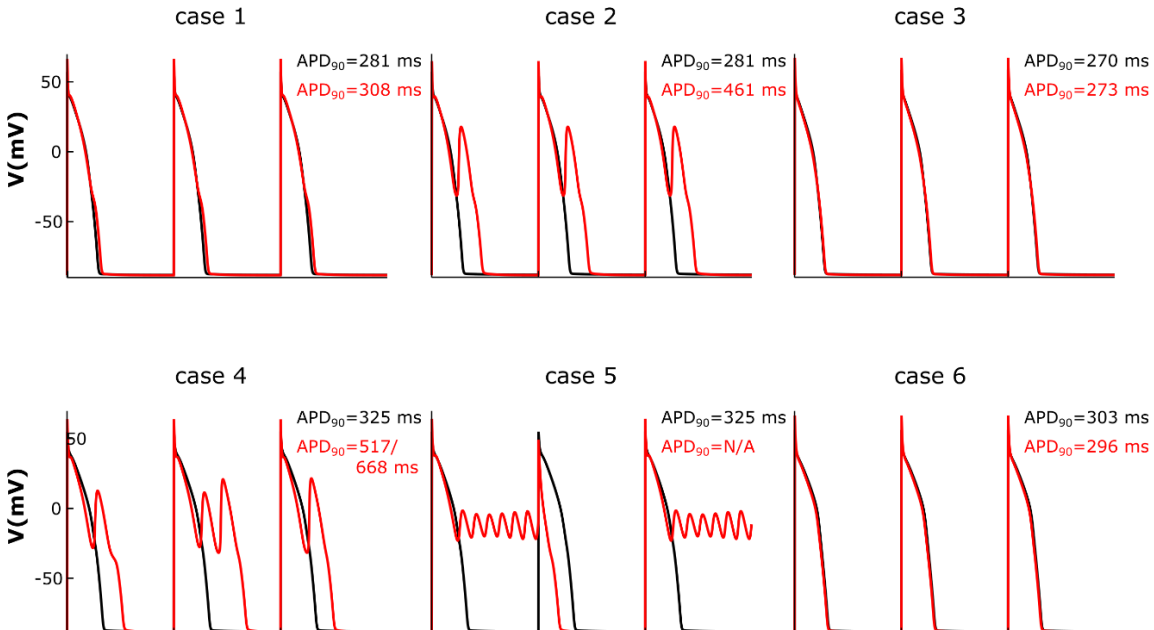

Figure 3.7 The effect of microstructure remodeling on membrane voltage and APs. The membrane potential of cells from cases 1-6 is plotted over time under both basal (black) and sympathetic stimulation (red) conditions. EADs emerged only under sympathetic stimulation in the cells where most LTCCs were either located in the T-tubules and lacking PDEs **(case 2)**, or they were in the surface membrane and experienced the effect of both β_2ARs and PDEs **(case 4)**. When most LTCCs were located in the bulk of the sarcolemma and were not associated with PDEs **(case 5)**, the cells were not able to repolarize and remained in an oscillatory state until the next stimulus was applied.

3.3.5 Effects of de-tubulation and β_2AR loss on APD_{90}

Lastly, we analyzed how gradual changes in the amount of de-tubulation as well as β_2AR and PDE signaling localization affect APD_{90} and EAD development. The heatmaps in Figure 3.8 were plotted in order to quantify how each of these variables impacts APD_{90} and EAD formation. The results demonstrate that EADs occurred only under adrenergic stimulation. Moreover, the loss of PDE control of cAMP in the dyadic space also contributed to the emergence of EADs.

No EADs formed when only 25% of the β_2ARs were present. When 50% of the β_2ARs were present EADs emerged either in fully de-tubulated cells, or in cells that lacked more than 20% of their PDE. In all the other cells, APDs appeared to increase proportionally to PDE and tubulation loss but no arrhythmogenic triggers were observed. The same trend was detected when the amount of functional β_2AR molecules was increased to 75%. In this case, we observed more frequent EAD

emergence, while the presence of intact tubulation and PDE had a protective effect. When all β_2ARs were present and functional, the model generated membrane potential oscillations for most cells that were lacking more than 60% of their initial T-tubules. EADs were obtained in almost all other cases, except the one in which tubulation was intact and at least 90% of PDEs were present. Thus, the presence of PDE molecules had a protecting effect, opposing APD_{90} prolongation and in some cases inhibiting EAD development.

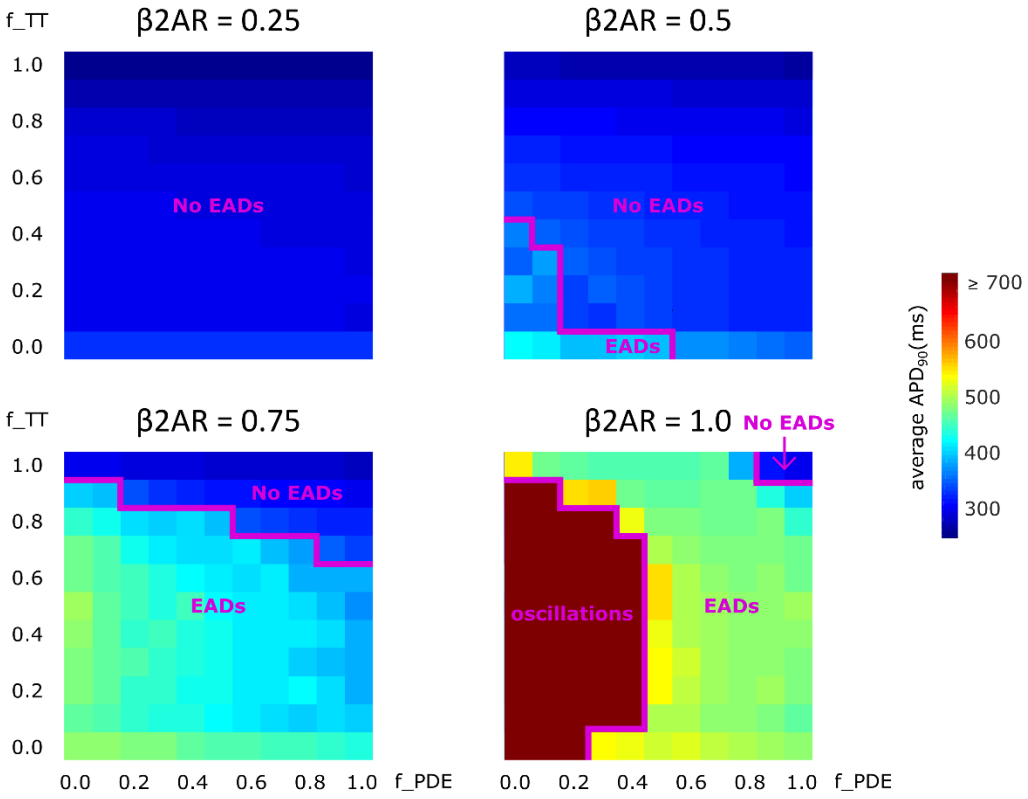

Figure 3.8 The effect of microstructure remodeling on APD_{90} and EAD emergence. Heatmaps of the average APD_{90} under sympathetic stimulation for 4 fixed values of the f_B2AR parameter. The cells range from intact (f_TT=1.0) to fully de-tubulated (f_TT = 0.0), and PDEs range from present and fully functional (f_PDE = 1.0) to completely absent (f_PDE = 0.0). EAD occurrence and oscillation behavior were also represented.

3.4 Discussion

3.4.1 Findings and Significance

Because HF electrophysiological remodeling is such a complex phenomenon, for the purpose of this computational study we used simulations to model and integrate only the structural changes described above. There are multiple other aspects described in Limitations that could be introduced in subsequent studies. Thus, the goal of this project was to elucidate the mechanisms by which subcellular changes in cardiac myocytes lead, via altered LTCC function, and under adrenergic stimulation, to the generation of cellular-level triggers of arrhythmia in human HF. To accomplish this goal, we developed a new ventricular myocyte computational approach that integrated various known characteristics of HF and allowed us to vary their severity. The model included the effects of microdomain remodeling on LTCC as in study by Sanchez and colleagues [15], as well as novel developments incorporating β_2AR stimulation, and arrhythmogenic remodeling of β_2 adrenergic signaling, as well as impaired control of cAMP levels due to altered PDE localization. We found that redistribution of the LTCCs combined with an enhanced phosphorylation of the channel due to abnormally high cAMP levels caused increases in LTCC current magnitude and duration. This resulted in AP prolongation and the development of single EADs, multiple EADs, or oscillations, depending on the amount of remodeling present.

3.4.2 Transverse T-tubules Loss in HF

The T-tubule system plays a vital role in normal ventricular cell function. Its structure and distribution are responsible for the rapid electric excitation, and the initiation and synchronous

triggering of Ca^{2+} release from the sarcoplasmic reticulum. The increase in Ca^{2+} levels throughout the cytoplasm leads to the coordinated contraction of all contractile units inside a cell [35]. Scanning ion conductance microscopy (SICM) and fluorescence staining experiments have shown that ventricular myocytes obtained from HF patients are characterized by a decrease in T-tubule density [12], [35]. This change in surface topography has been shown to take place gradually as the cardiac muscle transitions from hypertrophy to HF and to have a negative impact of excitation-contraction coupling [35]. Song and colleagues proposed that this deleterious effect is due to the reorganization of subcellular microdomains, which force RyRs to decouple from their partner LTCC and become orphaned. Thus Ca^{2+} ions flowing through the LTCCs fail to bind to RyRs and do not cause further Ca^{2+} release from the SR [36]. Other studies have shown that in HF, the loss of T-tubule microdomains is usually complemented by a spatial redistribution of LTCCs from the T-tubule membrane to the bulk of the sarcolemma, where they experience a different signaling environment [15]. Finally, work by Kawai and colleagues [37] and Bryant and colleagues [34] showed that complete myocyte de-tubulation is associated with reduction in I_{CaL} and shortening of APD. Taken together, the findings of these previous experimental studies suggest that altered LTCC function is a likely candidate for the mechanism linking T-tubule microdomain loss to the emergence of arrhythmogenic triggers in ventricular HF myocytes.

A novel aspect of our simulation approach lies in the fact that instead of creating a single model, by varying the amount of remodeling we obtained a family of models which allowed us to get an accurate depiction of the implications of T-tubule and cAMP compartmentalization loss in HF. By using this approach, we were able to analyze the effects of T-tubular loss alone, as well as in conjunction with a few other pathophysiological changes previously observed in HF in a setting that

resembled the progression of the disease. Because our study showed an increase in I_{CaL} and APD due to de-tubulation, it appears that our results are at odds with the results by Kawai et al., [37] and Bryant et al. [14]. However, that is not the case. The difference in our results comes mainly from the way we define de-tubulation and the exact distribution of channels between the T-tubular and the bulk of the sarcolemma. In our study, we view T-tubular microdomain disruption as a gradual process which slowly advances as HF progresses, similar to the changes that the myocytes from the above-mentioned studies undergo after coronary artery ligation (CAL). We are not trying to reproduce the data from a specific phase of the disease, as that would be impossible without introducing all the aspects of HF electrophysiological remodeling, but rather analyze the specific changes caused by gradual de-tubulation and cAMP re-distribution. If we compare one of our myocyte models constructed using the same ratio of channels in the T-tubular membrane vs. the bulk of the sarcolemma as in the CAL myocytes from the Bryant and colleagues, with what would be the equivalent of a healthy human myocyte in the study by Sanchez and colleagues [15], we get similar whole cell I_{CaL} current density (data not shown). However, because in their study de-tubulation is defined as a fast, chemical process which completely removes all T-tubular microdomain, and in our model de-tubulation is a slow process which allows the channels to relocate to the surface membrane, our results are different when we analyze de-tubulation. We could partially replicate their results if we completely eliminated the T-tubular component of I_{CaL}.

Furthermore, even though our results show an increase in I_{CaL} density due to HF when there are no experimental studies in humans showing that, we have to keep in mind that I_{CaL} peak and density seem to vary in HF from study to study [10], and in-silico studies don't always match the experimental ones [38] when it comes to this issue. However, our results do reflect the most

common change in I_{CaL} morphology caused by HF which is a slowing of the decay of the whole-cell current. Thus, our findings are consistent with the findings described above. They reproduce the change in I_{CaL} shape, add new insight about different stages of the disease, and highlight the existence of a threshold of T-tubule integrity that can predict the development of cellular level triggers of arrhythmia, as seen in Figure 3.8.

3.4.3 The role of β_2AR and PDE signaling localization loss in EAD development

Another hallmark of HF is βAR desensitization. Wright and colleagues showed, by combining a nanoscale SICM with a fluorescence resonance energy transfer (FRET) approach, that in healthy ventricular myocytes β_2AR-induced cAMP signals were highly localized within the T-tubular domain [19]. Heijman and colleagues used a computational model to describe in great detail the quantitative contribution of various molecules, including LTCCs, and the effects of the above mentioned signaling localization in adrenergic stimulation [22]. In HF myocytes, sympathetic stimulation of β_2AR appears to result in diffused, far reaching cAMP signals, which resembled those obtained via β_1AR stimulation. This suggests that similar to LTCCs, β_2ARs also change location from the T-tubular membrane to the surface membrane when tubulation is lost [18]. In addition, Lang and colleagues demonstrated that during end-stage HF, β_2AR stimulation leads to heterogeneities in APD and arrhythmogenic activity [39]. In our study, we were able to control the degree of both PDE and β_2AR loss of function and redistribution and to analyze how it influences the electrophysiological functioning of the myocytes in HF, and specifically, LTCC function.

Completely blocking β_2AR function in the model did not lead to abnormal LTCC current, nor to EAD occurrence. This is consistent with the fact that ligand binding failed to trigger a signaling cascade, and LTCCs were never phosphorylated (βAR desensitization). It also explains why adrenergic blockers work well as antiarrhythmic agents. When the β_2AR molecules were allowed to maintain partial functionality, but lost their localization, significant increases in LTCC current magnitude and APD_{90} as well as EAD development were observed. Moreover, when all β_2AR molecules were present, instead of EADs, the cells displayed an oscillatory behavior in which the membrane potential did not return to its baseline value. This is a biological phenomenon also recorded in isoprenaline perfused rabbit ventricular cardiomyocytes affected by long QT syndrome and thought to lead to sudden cardiac death [40]. These changes were opposed by the presence of PDE, which appears to have a protective, anti-arrhythmogenic effect. The new mechanistic insights presented here show that the binding of the ligand to functional, redistributed β_2ARs causes a cAMP signal propagation and amplification throughout the cell, which leads to the phosphorylation of multiple LTCCs across the cell membrane. Phosphorylated LTCCs have a higher open probability, which leads to a higher magnitude LTCC current, causing APD_{90} prolongation and EAD development.

3.5 Conclusion

Altered LTCC current is a major factor in the process linking microstructural remodeling to the increased risk of cellular arrhythmia triggers development in HF patients. Our results show that the disruption of subcellular microdomains and the redistribution of LTCCs, PDEs and β2ARs cause a higher-magnitude and longer-lasting LTCC current, which delays cellular repolarization. APs

are thus prolonged and upon sympathetic stimulation, EADs may arise. These findings provide important insight into the mechanism underlying the development of cellular level triggers of arrhythmia in human HF and suggest β2ARs and PDEs as possible targets for future therapies and preventive treatments of ventricular arrhythmia.

3.6 Limitations

Our study has several limitations. HF remodeling is a very complex process with many unknowns. Our model thus had various assumptions. First, in the lack of experimental evidence otherwise, we assumed that the LTCCs remaining in the T-tubular membrane in HF are fully functional; even super-resolution scanning patch clamp studies such as the one presented by Sanchez et. al [15] cannot measure LTCC activity deep inside the T-tubule system. Secondly, in order to be able to draw mechanistic insight, we limited the degrees of freedom of our model by keeping both the number of LTCCs as well as their conductance constant. This may be at odds with observations by Bryant et. al which suggest that in heart failure, myocytes show a decrease in the number of LTCCs and an increase in their activity [34]. Also, our model focused exclusively on the activity of LTCC channels in HF, and did not include changes in other currents such as $I_{Na,L}$, I_{Ks} and I_{Kr} which are also affected by HF remodeling. Due to limited data on PKA-mediated phosphorylation of LTCCs in HF, by using only the electrophysiological and not the signaling module of the model Heijman model [22], we had to make approximations regarding the fraction of channels phosphorylated under baseline conditions and under adrenergic stimulation. Moreover, our

study focuses exclusively on the effect of microdomain loss on β_2AR, based on previous studies showing that HF leads to the re-distribution of these receptors which in turn affects the activity of LTCCs [18], although β_1AR stimulation is the major receptor mediating the effects of sympathetic stimulation of the heart. This could be explored in greater depth in future work. CaMKII-dependent phosphorylation of different channels was also included in the model, but as our study focused solely on the effect of sympathetic stimulation and PKA-dependent phosphorylation of LTCCs, CaMKII remodeling was not implemented. Since PDE3 acts as a negative feedback-loop for cAMP level control, the model assumed that PDE3-mediated cAMP degradation is a process activated by PKA and thus PDE should only be active under sympathetic stimulation when PKA levels are increased. Also, only the activity of PDE3 was modeled and PDE signaling localization loss was modeled to be directly proportional to T-tubular loss. In further studies, the model will account for different isoforms of PDEs as decribed by Zhao et al. [30]. Lastly, the present study focused on single cell behavior; thus, it is possible that the results can be modulated by the effect of cell coupling on the susceptibility of cells to form EADs, as described by Xie and colleagues [35]

Chapter 4: Altered L-type Calcium Channels Function Differentiates between Ischemic and Dilated Cardiomyopathies.

This work is part of a study submitted for publication.

4.1 Introduction

As structural heart diseases such as myocardial hypertrophy progress from an early form towards advanced HF, patients acquire a higher risk of developing arrhythmias and sudden cardiac death. Although for decades, LTCCs have been suggested as a possible contributor to an abnormal cardiac function in HF, not much attention has been given to their regional variation within a cell, nor to their functional variation across different disease etiologies. Several studies have shown that T-tubular microdomains are lost in HF [41], while base-line whole cell I_{CaL} stays unchanged [33], [32], [42]. This suggests that LTCCs in HF may be hyperphosphorylated in order to compensate for channel loss. In fact, studies on single channel recordings by other authors have shown an increase in LTCC open probability in human HF [15], which could be explained by a higher phosphorylation of the channel. Furthermore, while in ischemic cardiomyopathies (ICM), this elevated open probability has

been observed on channels located in the T-tubular membrane, in dilated cardiomyopathies (DCM) the channels in the bulk of the sarcolemma show a higher open probability. This microdomain-specific abnormality in LTCC behavior was found to depend on whether the channels were hyperphosphorylated by PKA or by CaMKII.

The goal of this study was to explore the mechanisms by which HF-induced changes in phosphorylation patterns due to PKA in the ICM case and CAMKII in the DCM case combined with an altered LTCC distribution to cause an abnormal LTCC current which promotes the development of EADs in human ventricular myocytes. To this end, we employed three different ionic models to analyze the LTCC channel behavior as well as AP generation in silico. Our results show valuable insight into the processes that favor the development of cellular arrhythmogenic triggers in HF patients as well as the effect of these triggers at whole-organ level.

4.2 Methods

4.2.1 Modeling Methodology

The O'Hara-Rudy ionic model[43] was used to represent the electrophysiology of healthy human ventricular cardiomyocytes. Additionally, we developed both endocardial and epicardial models for three different cases (control, DCM and ICM), in order to perform single-cell simulations. Whole-cell LTCC current behavior, APs and the possible emergence of cellular-level triggers of arrhythmias were studied. The ionic models were then used in an MRI-derived, anatomically realistic, healthy human ventricular model, to evaluate if the EADs observed in single-cell simulations would develop into reentrant arrhythmias at organ-level.

4.2.2 Single Cell Modeling Methodology

As previously mentioned, the O'Hara-Rudy ionic model[43] was used to model action potentials in healthy human ventricular cardiomyocytes. We introduced a number of changes in the formulation of the human LTCC current, in order to represent the subcellular remodeling observed in different etiologies of cardiomyopathy. Myocytes from dilated human hearts were modeled by incorporating the changes in the ionic model described in previous work[15]. To model cells from ischemic human hearts, we introduced modifications based on the experimental data from the Gorelick lab. Specifically, we introduced a parameter defining T-tubular integrity and set its value to 0.65. Next, we allowed a fraction of 0.45 LTCCs within a cell to maintain their position within the T-tubular membrane, while the remaining 0.55 fraction of channels were relocated to the bulk of the sarcolemma. These values were computed using the data describing T-tubular density and regularity and channel occurrence and are explained in more detail in the following sections. As observed experimentally, there was an increase in P_o of LTCCs on the non T-tubular sarcolemma for the DCM etiology, and in the T-tubule membrane in the ICM case. While in DCM myocytes this change occurs due to phosphorylation of LTCCs by CaMKII, in ICM myocytes PKA appears to be responsible for the enhancement of LTCC phosphorylation. Therefore, we introduced PKA into our ICM cardiomyocyte model and allowed it to interact with the LTCCs present in the T-tubular domain. Similar to the O'Hara-Rudy human ventricular model combined with the electrophysiological module of the Heijman beta adrenergic model[22] described previously[23], when PKA phosphorylated an LTCC, the current through that channel was increased by a factor of 2.5 and the gating parameters

were updated. However, while all LTCCs in the non T-tubular sarcolemma were assumed to operate in the CaMKII-phosphorylated mode in DCM, only a fraction of 0.7 LTCCs in the T-tubules in ICM were set to function in the PKA-phosphorylated mode, in order to match the Po observed experimentally, as described below.

Apart from the remodeling observed in the LTCC current, all the other ionic changes described in the study by Sanchez-Alonso and colleagues[15] representing DCM cardiomyopathy were also included in the model of the ICM etiology. Thus, within the model, the formulation of the LTCC current is what differentiates between the ICM and DCM cases.

Finally, we represented the electrophysiological differences in ionic remodeling between epi- and endocardial cells in each etiology using the same approach as the study by Elshrif and colleagues [38].

Using the three models described above (control, DCM and ICM), for both endocardial and epicardial myocytes, we performed single-cell simulations using both a voltage-clamp protocol to analyze the whole-cell LTCC current behavior, and a pacing protocol in order to observe differences in action potentials and the possible emergence of cellular-level triggers of arrhythmias such as EADs.

4.2.3 Accounting for T-tubular Loss and LTCC Redistribution in Ischemic Cardiomyopathies

The modified O'Hara-Rudy model was used in both the Sanchez-Alonso et al. study[15] and our current study to represent the control case had intact T-tubular domains. In order to model the loss of T-tubules observed experimentally in ischemic cardiomyopathies we introduced the parameter TTD encoding for T-tubular integrity. We set its value to be 0.65 using the equation:

$$\mathrm{TTD} = \left(\frac{\text{TT density in ICM}}{\text{TT density in control}} + \frac{\text{Z groove ratio in ICM}}{\text{Z groove ratio in control}}\right) \cdot \frac{1}{2}$$

Then, we introduced two new parameters encoding for the distribution of LTCCs between the T-tubular region and the Non T-tubular sarcolemma domains. Thus, the ratio between the channels located in the T-tubular domain to the channels located in the Non T-tubular sarcolemma was found to be 0.8 using the equation:

$$\frac{\#\text{ channels in TT}}{\#\text{ channels in non T} - \text{tubular sarcolemma}} = \frac{\text{Percentage of recordings with LTCCs on the TT}}{\text{Percentage of recordings with LTCCs on the Non T} - \text{tubular sarcolemma}}$$

Therefore, a fraction of approximately 0.45 of LTCCs within a cell were located on the T-tubular membrane, while the remaining 0.55 were relocated to the Non T-tubular sarcolemma.

As experimental evidence from human myocytes has indicated that remodeling has no effect on the peak of the LTCC current[43], we adjusted the whole cell LTCC current to match that of the control in terms of magnitude, by multiplying it with a correction factor.

4.2.4 Setting the Fraction of LTCCs in ICM T-tubules to be Phosphorylated by PKA

Similar to the Sanchez et. al study[15], we used a stochastic Markov formulation to model the single channel behavior and determine the appropriate fraction of channels which would undergo PKA phosphorylation in ICM T-tubules, in order to match the experimentally observed open probability value. We used the same 32 sates Markov model described in a previous study [15] to represent unphosphorylated channels. However, when phosphorylation by PKA was introduced, 32

additional equivalent states were created, all characterized by different gating kinetics as described in the O'Hara-Rudy model combined with the Heijman model[22], [23]. By stochastically simulating the behavior of 1000 channels at a voltage of -6.7mV, we determined that only a fraction of 0.7 LTCC channels need to be phosphorylated in order to match the desired open probability. This is different that the DCM model in which all channels in the non T-tubular sarcolemma were phosphorylated by CaMKII. After computing this fraction, we reverted the Markov model to the equivalent Hodgkin-Huxley formalism.

4.2.5 Whole-heart modeling approach

To evaluate whether EADs observed in the cell-level simulations would develop into reentrant arrhythmias in a human heart, we used our ICM, DCM and control ionic models for both endocardial and epicardial myocytes, and implemented them in an MRI-derived, anatomically realistic, healthy human ventricular model. The same model was utilized in a previous study[15], in which transmural electrophysiological differences (epi- vs. endo-) in the ventricles were represented by dividing the ventricular walls into an epi- and endocardial layers and using the corresponding ionic model for each region based on experimental data. Transmural conductivity was implemented as a gradient between the epi- and endocardial surfaces based on experimental data from human left ventricle[44], as done in a previous study[15]. A computational mesh with resolution of $<300\mu m$ was generated and fiber orientation was assigned using a rule-based approach[45]. Stimuli were applied at the apex of the ventricles using a 2.5 mm virtual electrode. Two initial stimuli were delivered at 1s intervals, followed by a pause in stimulation representing two skipped heart beats, similar to our previous approach in cell-level simulations[15]. After 4 seconds from the beginning of the simulation,

regular pacing at 1Hz was resumed. The simulations were performed using the CARP software package[46], [47].

4.3 Results

4.3.1 Cellular Level Computational Modeling Predicts Abnormal LTCC behavior in both DCM and ICM etiologies

In single-cell voltage clamp simulations using either the endocardial or epicardial myocyte models described in the Methods section, stepping the membrane voltage from -96.7 mV to -6.7mV, as in the experimental protocol, led to an influx of Ca^{2+} ions into the cell similar in magnitude across all the three cases (control, DCM and ICM), which agrees with previous findings[32], [33], [42]. The rate at which these currents decayed however, varied between the three cases, with the control case displaying the fastest rate, and the DCM being the slowest. This suggests that LTCC current could be a potential cause of action potential prolongation and its destabilization in the ICM and DCM models. Examining the $I_{Ca,L}$ current through the channels located exclusively in the T-tubular microdomains, we found that its values in the control and ICM model myocytes were nearly identical in terms of magnitude, while the magnitude of the $I_{Ca,L}$ current in DCM was significantly lower. Thus, although there are fewer channels in the TT domain in both cardiomyopathy etiologies, in ICM myocytes, the TT operating under PKA-phosphorylation mode compensate for the loss of channels due to LTCC relocation. This was expected since phosphorylation was characterized by a 2.5 increase of the current

through the LTCC channels. A surprising result of these simulations was, however, that all currents in the T-tubular membrane for the three myocyte cases showed very similar decay rates. While this was expected for the control and DCM cells, in which the channels are not phosphorylated, it was an unexpected result from the ICM myocyte model, in which channels in the T-tubular domains experience the effect of PKA phosphorylation and thus have a higher P_o. This result can be explained by the fact that LTCCs experience both voltage and Ca^{2+} dependent inactivation, and that at hyperpolarized potentials such as -6.7 mV Ca^{2+} dependent inactivation is stronger than voltage dependent inactivation. Within the dyadic space, the high Ca^{2+} concentration rapidly inactivates the channels in all pathology cases and keeps a close control of channel opening, thus leading to currents with very similar decay rates. On the other hand, in the non T-tubular sarcolemma microdomain the Ca^{2+} dependent inactivation is lower; since Ca^{2+} does not accumulate as much, voltage dependent inactivation dominates, and thus all channels there display a slower decaying current than in T-tubules. This slower decay of $I_{Ca,L}$ is exacerbated in the DCM case by the phosphorylating effect of CaMKII on non T-tubular sarcolemma LTCCs leading to a higher-amplitude and a slower-decaying current.

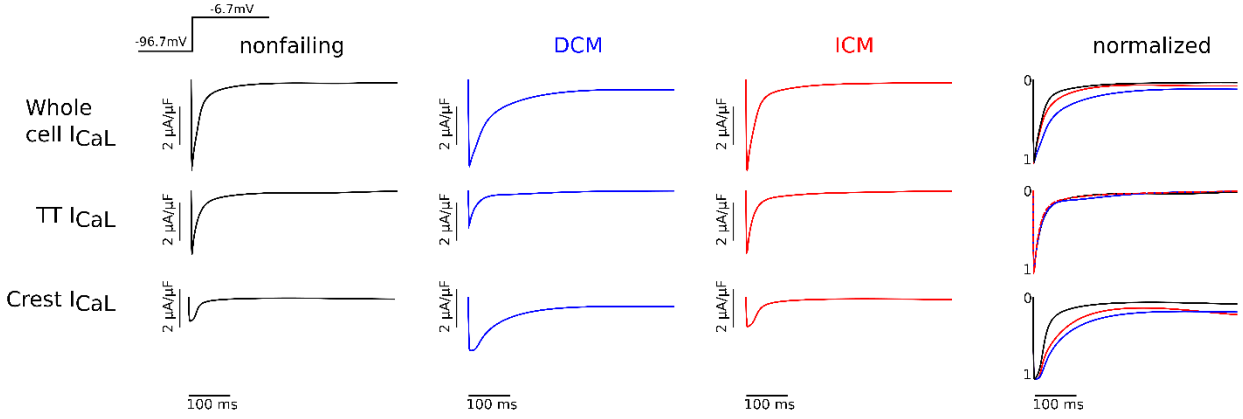

Figure 4.1 Overview of whole L-type calcium current model under voltage-clamp protocol. The LTCC current from the control (black), DCM (blue) and ICM (red) cases was plotted over time after the voltage was stepped from -96.7 to -6.7 mV. The currents were then normalized and plotted on the same graph, allowing us to compare their decay rates. The three rows represent the whole cell

LTCC current (first row), the LTCC current through the channels in the TT (second row) and the one through the channels from the non T-tubular sarcolemma (third row).

4.3.2 Single Cell Simulations Also Predict the Emergence of Cellular-Level Triggers of Arrhythmia in both DCM and ICM Etiologies

When myocyte models were paced at 0.25Hz, simulation results demonstrated that the changes in LTCC kinetics described above lead to the emergence of early afterdepolarization (EADs) exclusively in the endocardial myocytes of ICM and DCM patients. Blocking the phosphorylating effects of PKA and CaMKII on LTCCs in the pathological cases led to the disappearance of the EADs under an identical protocol (Figure 4.2), which indicates that the two molecules play key roles in the development of cellular-level triggers of arrhythmia in cardiomyopathies.

Even though EADs can act as triggers of ectopic beats, their formation does not often result in the emergence of reentrant arrhythmias in the whole heart. Thus, we conducted organ-level simulation with the whole-heart ventricular models described in Methods to examine the conditions under which reentrant arrhythmias originate.

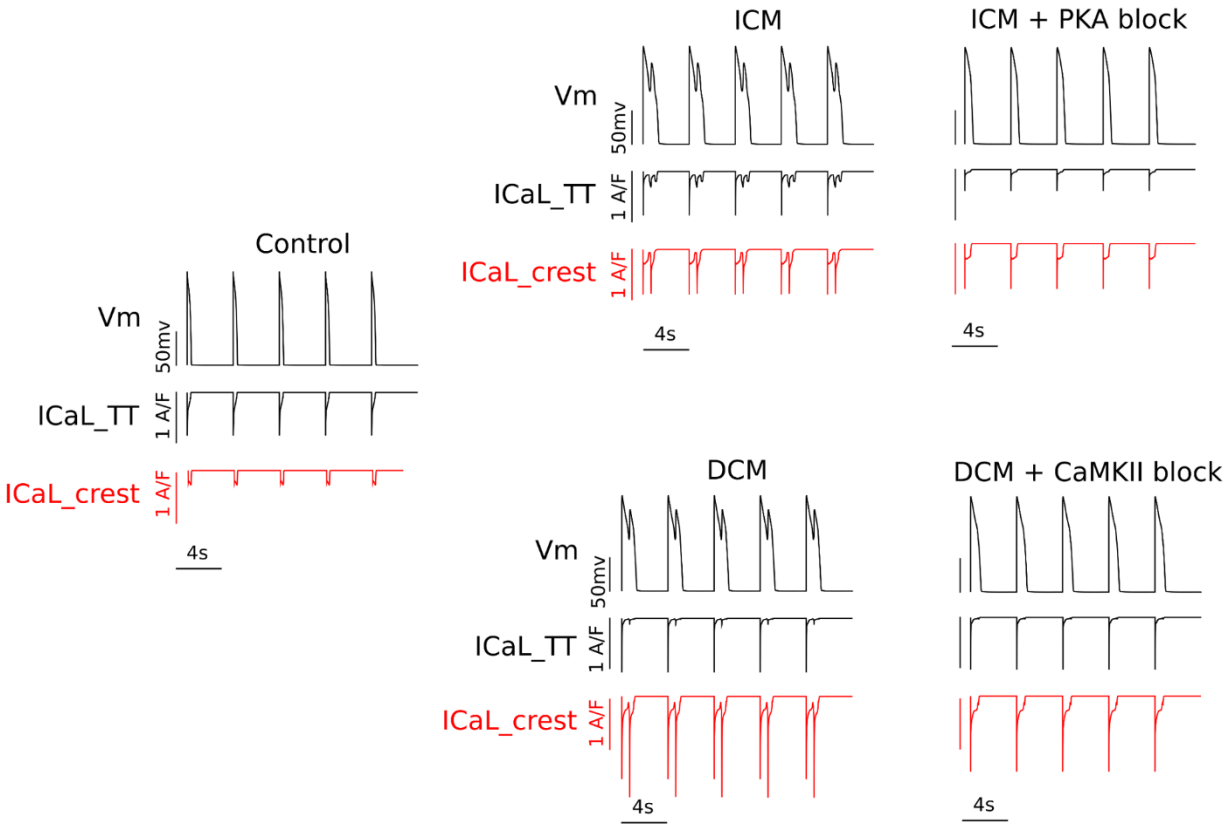

Figure 4.2 Comparison of membrane voltage and L-type Calcium current traces. The membrane voltage and corresponding L-type Calcium current traces were plotted over time when the model myocytes were paced at 0.25Hz. Models of myocytes from control, ischemic and dilated hearts are represented. For the ICM case, EADs were obtained when the LTCCs in the T-tubuless were phosphorylated by PKA (top row, left), but not when PKA activity was blocked (top row, right). Similarly, arrhythmogenic triggers developed in the DCM case when LTCCs from the non T-tubular sarcolemma were phosphorylated by CaMKII (bottom row, left), and not when CaMKII activity was blocked (bottom row, right). Changes in L-type Calcium current morphology, but not peak magnitude was observed when phosphorylation was blocked. However, changes in the amplitude of the current through the channels in both T-tubular membrane and non T-tubular sarcolemma were observed between the etiology cases.

4.3.3 Organ-scale Simulations Predict the Development of Arrhythmias in the DCM, but not in the ICM Cardiomyopathy

As in the single-cell simulations, arrhythmogenic activity in the whole-heart (see Methods for description) arose from the endocardial layer. The formation of arrhythmogenic triggers only in the ICM ventricles and of both arrhythmogenic triggers and reentrant arrhythmia in the DCM ventricles is illustrated in Figure 4.3. No arrhythmic events were observed in the control case. Action potential duration of the first two beats following stimulation was found to be significantly increased (compared to control) in both pathological cases. Skipping the subsequent two beats to facilitate EAD emergence, as done in previous work at cellular level[15], had no effect in the control ventricles but led to reentrant arrhythmia in the DCM heart model. In contrast, when we skipped two beats in the ICM ventricular model, we observed emergence of EADs only in a small island of tissue, and it did not develop into a reentrant arrhythmia.

Overall, our simulations showed how the loss of TT and the subsequent redistribution of LTCCs alters cellular action potential. EADs have been widely described in the literature [48], and our simulations demonstrating emergence of EADs in ICM and DCM cells are consistent with these studies (Figure 4.2).

In our DCM model, CaMKII phosphorylated LTCCs in the non T-tubular sarcolemma, resulting in an altered non T-tubular sarcolemma I_{CaL} compared to control, with a higher magnitude and a slower decay (Figure 4.1). These changes were the main cause for EAD emergence. In ICM, PKA phosphorylated LTCCs mostly in TT, however, TT I_{CaL} had the magnitude and kinetics of control (Figure 4.1), as the loss of LTCCs in this microdomain was compensated by the increase in Po through PKA phosphorylation of the channels remaining in TT. This suggest that the Ca^{2+} handling proteins associated with the TT such as Na^{+}-Ca^{2+}

exchanger, sarcolemmal Ca^{2+}-ATPase and the SR Ca^{2+} uptake pump are more efficient on TT than on the non T-tubular sarcolemma. This reveals new insights into the mechanism of HF, indicating how the location of LTCCs could be more important than their phosphorylation state.

Whole heart simulations demonstrated that LTCC alterations in DCM have worse consequences at the organ level (reentrant arrhythmias) than LTCC alterations in ICM (Figure 4.3). This points to the subcellular location as being a key player in the process of LTCCs becoming the trigger of arrhythmogenic events. When LTCCs are located in TT, the machinery of the cell in this microdomain can precisely control calcium influx and even compensate for channel loss with an increase in P_o. However, when LTCCs are located in the non T-tubular sarcolemma, balance is easily disrupted, and an increase in channel number there leads to EADs (as shown by ICM simulations). If this is accompanied by an increase in P_o (DCM simulations), electrophysiological disturbances will progress to reentrant arrhythmias.

our simulations demonstrated that subtle differences in microdomain remodeling between ICM and DCM cardiomyopathies lead to very different electrophysiological outcomes at the whole-heart level. Specifically,

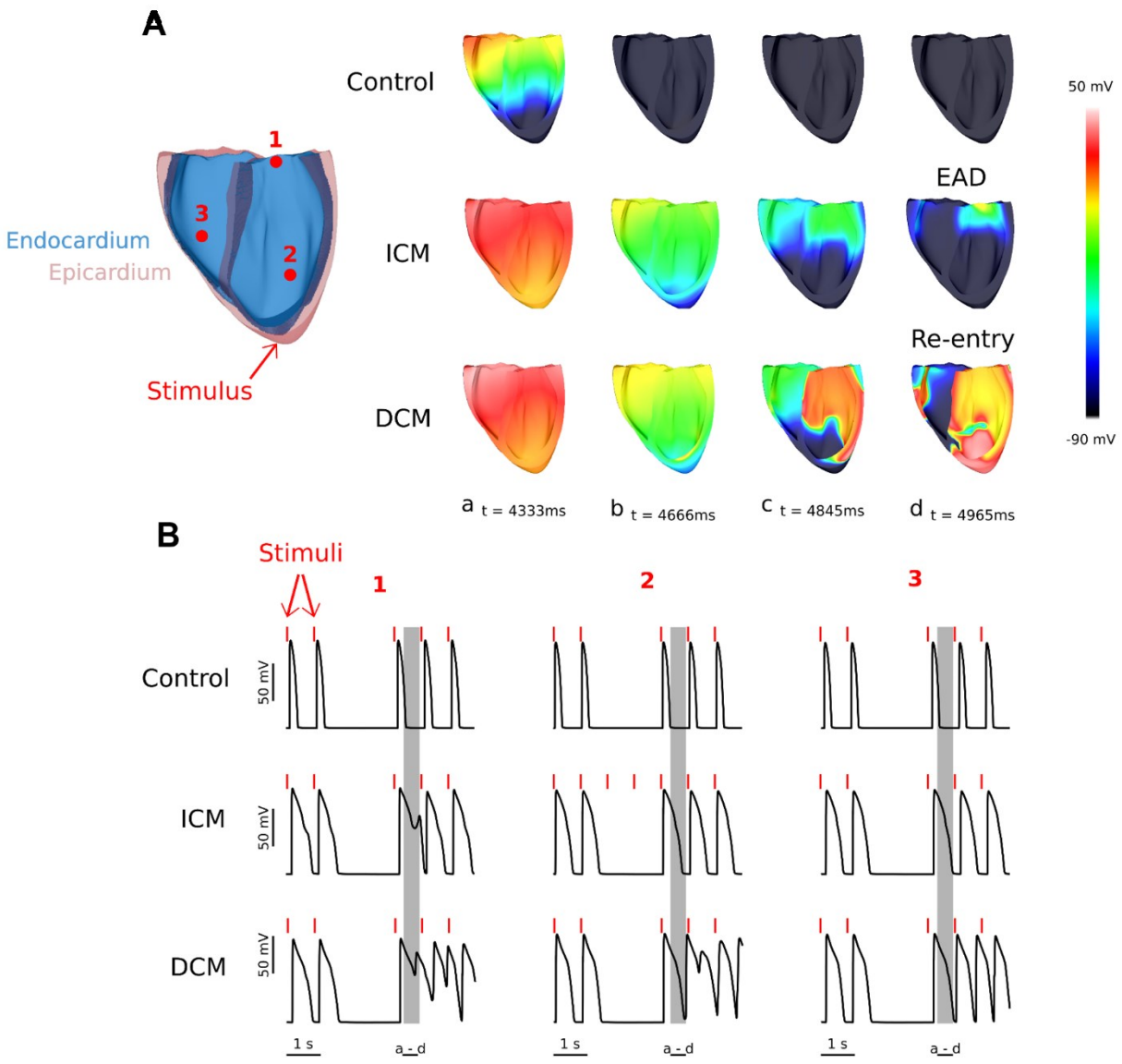

Figure 4.3 Graphical representation of the whole heart simulations. (A) The voltage maps from 4 different points in time were plotted for the three cases (Control, ICM, DCM). A short depolarization between two consecutive stimuli was recorded in the ICM heart, while a reentrant arrhythmia was obtained in the DCM organ. **(B)** The membrane potential was recorded from three different virtual electrodes in the ventricles and displayed. In the ICM case, an island of tissue displayed a synchronous single EAD following the stimulus after the skipped 2 beats. In the DCM case, both singular and multiple EADs were recorded in one or more beats after the skipped ones.

4.4 Discussion

Because abnormal Ca^{2+} signaling is a known contributor to the pathology of human HF, its signaling pathways are typically targeted in current therapies for HF. In this study, we combined experimental data from the Gorelick lab with our computational models in order to gain new insights into the emergence of arrhythmogenic triggers and re-entrant arrhythmia in different human HF etiologies. Specifically, we analyzed the two different pathways observed in the progression of ICM and DCM: a pathological activation of CaMKII in DCM cardiomyopathies and of PKA in ICM cardiomyopathies. Our research showed how sub-cellular microstructure changes in HF can lead to electrical dysfunction at organ level, and how the phosphorylation state of LTCCs in different microdomains can trigger arrhythmogenic events in the whole heart.

4.4.1 The Etiology of the Disease Determines Microdomain-dependent Phosphorylation of LTCCs either by PKA or CaMKII

The two main kinases known to modulate LTCC activity in human cardiomyocytes are PKA and CaMKII [49]. The behavior of LTCCs is regulated by the kinases' interactions with the C-terminal of the α subunit of the channel [50], [51]. The progression of HF is usually associated with various changes in PKA and CaMKII activity, including oxidation, altered expression and post-translational changes. A previous study by Sanchez-Alonso and colleagues [15] showed that an increase in the activity of CaMKII is responsible for the changes observed in human DCM myocytes, including the high P_o of LTCCs relocated to the bulk of the sarcolemma. Since CaMKII activity does not appear to be enhanced in ICM cardiomyocytes, the culprit behind the increase in P_o of LTCCs located in the T-tubular part of the sarcolemma is likely to be PKA. This hypothesis is supported in a study by Han and colleagues [52] which shows that post-translational modifications can lead to an increase in PKA

activity and a subsequent increase in LTCC phosphorylation. When we incorporated these separate pathways in our computational models, we obtained similar results in cellular-level simulations of DCM and ICM cardiomyocytes, and different behavior at organ scale.

4.4.2 The Outcome of the Sub-cellular LTCC Distribution on the Whole Heart is Revealed by Simulations

Our simulations showed how the loss of T-tubules and the subsequent redistribution of LTCCs alters cellular action potential. EADs have been widely described in the literature[48], and our simulations demonstrating emergence of EADs in ICM and DCM cells are consistent with these studies (Figure 4.2).

In our DCM model, CaMKII phosphorylated LTCCs in the non T-tubular sarcolemma, resulting in an altered non T-tubular sarcolemma I_{CaL} compared to control, with a higher magnitude and a slower decay (Figure 4.1). These changes were the main cause for EAD emergence. In ICM, PKA phosphorylated LTCCs mostly in T-tubules, however, T-tubular I_{CaL} had the magnitude and kinetics of control (Figure 4.1), as the loss of LTCCs in this microdomain was compensated by the increase in Po through PKA phosphorylation of the channels remaining in TT. This suggest that the Ca^{2+} handling proteins associated with the T-tubules such as Na^{+}-Ca^{2+} exchanger, sarcolemmal Ca^{2+}-ATPase and the SR Ca^{2+} uptake pump[53] are more efficient on the T-tubular membrane than on the non T-tubular sarcolemma. This reveals new insights into the mechanism of HF, indicating how the location of LTCCs could be more important than their phosphorylation state.

Whole heart simulations demonstrated that LTCC alterations in DCM have worse consequences at the organ level (reentrant arrhythmias) than LTCC alterations in ICM (Figure 4.3).

This points to the subcellular location as being a key player in the process of LTCCs becoming the trigger of arrhythmogenic events. When LTCCs are located in TT, the machinery of the cell in this microdomain can precisely control Ca^{2+} influx and even compensate for channel loss with an increase in P_o. However, when LTCCs are located in the non T-tubular sarcolemma, balance is easily disrupted, and an increase in channel number there leads to EADs (as shown by ICM simulations). If this is accompanied by an increase in P_o (DCM simulations), electrophysiological disturbances will progress to reentrant arrhythmias.

4.4.3 Clinical Implications

Due to the differences observed in the progression of different etiologies of HF, the prognosis and survival odds of patients suffering from HF may benefit from an early diagnosis of the etiology of the disease. We have shown that different microdomain changes at cellular level result in different pathologies at organ scale. Physicians may take advantage of this result and make informed choices to target specific molecules in their treating of a patient, once they know the source of the disease.

Chapter 5: Conclusion and Future Directions

The overarching goal of this thesis' work was to explore a novel set of mechanisms by which sub-cellular microdomain remodeling leads to an increased risk of lethal arrhythmias in human HF patients. Specifically, using biophysically detailed computer models of human cardiomyocytes, we have shown that altered LTCC function is a possible cause of EAD emergence at cellular level and is mechanistically linked to increased arrhythmia risk in at least one HF etiology.

In Chapter 3, we have presented a comprehensive study into the effects of T-tubular microdomain loss in HF on LTCC behavior. We have demonstrated that the subpopulations of LTCCs which are relocated from the t-tubular membrane to the bulk of the sarcolemma are forced to operate in a non-native signaling domain which causes them to lose vital function control. The consequence of this change was an increase in I_{CaL} magnitude and duration which in turn, caused AP prolongation and in some cases EAD development.

In Chapter 4 we went one step further, and evaluated the effects of remodeling in two different cardiomyopathy etiologies, from sub-cellular to organ level. We showed that while at cellular level, altered LTCC function caused by an increased PKA activity in ICM and an increased CAMKII activity in DCM lead to similar outcomes in terms of AP prolongation and EAD formation, at organ level, the same changes have different results, only causing reentrant arrhythmias in the DCM ventricles.

These discoveries have several important implications. First, these simulations may be useful in understanding the progression of HF, and how different pathologies can result from changes in

microdomains at the single cell level. Secondly, our work may be useful in informing choice of anti-arrhythmic therapies and strategies specific to patient's pathophysiology and type of underlying arrhythmic substrate. Specifically, our results highlight the importance of phosphorylated LTCC in the development of arrhythmias, suggesting that treatments targeting phosphorylated LTCCs as well as B2ARs and PDEs could be the key to HF prognosis improvement. Lastly, our study proves once more the usefulness of detailed computational models in providing valuable insights into clinically relevant mechanisms of arrhythmogenesis. The scope of our studies, spanning multiple levels from molecular to whole-organ, allowed us to gain knowledge of phenomena which would be difficult, if not impossible, to observe in experimental settings. However, empirical data is essential in developing accurate computational models. Thus, as more data from experiments becomes available, it should be included in our present state-of-the-art models in order to further our understanding and treatment of HF in the future.

Reference List

[1] P. Harris, "The definition of heart failure," *Eur. Heart J.*, vol. 4, no. 8, p. 600, 1983.

[2] R. V. Luepker, "Epidemiology of heart failure," *Congest. Hear. Fail. Card. Transplant. Clin. Pathol. Imaging Mol. Profiles*, no. March, pp. 93–102, 2017.

[3] D. Mozaffarian *et al.*, *Heart disease and stroke statistics-2016 update a report from the American Heart Association*, vol. 133, no. 4. 2016.

[4] G. F. Tomaselli and D. P. Zipes, "What causes sudden death in heart failure?," *Circ. Res.*, vol. 95, no. 8, pp. 754–763, 2004.

[5] W. G. Stevenson, "Predicting Sudden Death Risk for Heart Failure Patients in the Implantable Cardioverter-Defibrillator Age," *Circulation*, vol. 107, no. 4, pp. 514–516, 2003.

[6] G. I. Fishman *et al.*, "Sudden cardiac death prediction and prevention: Report from a national heart, lung, and blood institute and heart rhythm society workshop," *Circulation*, vol. 122, no. 22, pp. 2335–2348, 2010.

[7] P. S. Azevedo, B. F. Polegato, M. F. Minicucci, S. A. R. Paiva, and L. A. M. Zornoff, "Cardiac Remodeling: Concepts, Clinical Impact, Pathophysiological Mechanisms and Pharmacologic Treatment," *Arq. Bras. Cardiol.*, pp. 62–69, 2016.

[8] M. M. Elshrif, P. Shi, and E. M. Cherry, "Representing Variability and Transmural Differences in a Model of Human Heart Failure," *IEEE J. Biomed. Heal. Informatics*, vol. 19, no. 4, pp. 1308–1320, Jul. 2015.

[9] A. D. Loucks, T. O'Hara, and N. A. Trayanova, "Degradation of T-Tubular Microdomains and Altered cAMP Compartmentation Lead to Emergence of Arrhythmogenic Triggers in Heart Failure Myocytes: An in silico Study," *Front. Physiol.*, vol. 9, no. December, pp. 1–12, 2018.

[10] G. F. Tomaselli and E. Marban, "Electrophysiological remodeling in hypertrophy and heart failure," *Cardiovasc. Res.*, vol. 42, no. 2, pp. 270–283, 1999.

[11] M. Rubart and D. P. Zipes, "Mechanisms of sudden cardiac death," *J. Cllinical Investig.*, vol. 115, no. 9, pp. 2305–2315, 2005.

[12] A. R. Lyon *et al.*, "Loss of T-tubules and other changes to surface topography in ventricular myocytes from failing human and rat heart," *Proc. Natl. Acad. Sci. U. S. A.*, vol. 106, no. 16, pp. 6854–6859, 2009.

[13] A. V. Zima, E. Bovo, S. R. Mazurek, J. A. Rochira, W. Li, and D. Terentyev, "Ca handling during excitation-contraction coupling in heart failure," *Pflugers Arch. Eur. J. Physiol.*, vol. 466,

no. 6, pp. 1129–1137, 2014.

[14] S. M. Bryant, C. H. T. Kong, J. Watson, M. B. Cannell, A. F. James, and C. H. Orchard, "Altered distribution of I<inf>Ca</inf> impairs Ca release at the t-tubules of ventricular myocytes from failing hearts," *J. Mol. Cell. Cardiol.*, vol. 86, pp. 23–31, 2015.

[15] J. L. Sanchez-Alonso *et al.*, "Microdomain-Specific Modulation of L-type Calcium Channels Leads to Triggered Ventricular Arrhythmia in Heart Failure," *Circ. Res.*, vol. 44, no. July, p. CIRCRESAHA.116.308698, 2016.

[16] D. M. Bers, "Calcium cycling and signaling in cardiac myocytes.," *Annu. Rev. Physiol.*, vol. 70, pp. 23–49, 2008.

[17] V. Timofeyev *et al.*, "Adenylyl cyclase subtype-specific compartmentalization: Differential regulation of L-Type Ca2+current in ventricular myocytes," *Circ. Res.*, vol. 112, no. 12, pp. 1567–1576, 2013.

[18] P. N. Viacheslav O. Nikolaev, Alexey Moshkov, Alexander R. Lyon, Michele Miragoli and J. G. Helen Paur, Martin J. Lohse, Yuri E. Korchev, Sian E. Harding, "B2-Adrenergic Receptor Redistribution in Heart Failure Changes cAMP Compartmentation," *Science (80-.).*, vol. 327, no. March, pp. 1653–1657, 2010.

[19] P. T. Wright *et al.*, "Caveolin-3 regulates compartmentation of cardiomyocyte beta2-adrenergic receptor-mediated cAMP signaling," *J. Mol. Cell. Cardiol.*, vol. 67, pp. 38–48, 2014.

[20] J. Heijman, P. G. A. Volders, R. L. Westra, and Y. Rudy, "Local control of ??-adrenergic stimulation: Effects on ventricular myocyte electrophysiology and Ca 2+-transient," *J. Mol. Cell. Cardiol.*, vol. 50, no. 5, pp. 863–871, 2011.

[21] T. O'Hara, L. Virág, A. Varró, and Y. Rudy, "Simulation of the undiseased human cardiac ventricular action potential: Model formulation and experimental validation," *PLoS Comput. Biol.*, vol. 7, no. 5, 2011.

[22] J. Heijman, P. G. A. Volders, R. L. Westra, and Y. Rudy, "Local control of β-adrenergic stimulation: Effects on ventricular myocyte electrophysiology and Ca2+-transient," *J. Mol. Cell. Cardiol.*, vol. 50, no. 5, pp. 863–871, May 2011.

[23] T. O. Hara and Y. Rudy, "Arrhythmia formation in subclinical (' silent ') long QT syndrome requires multiple insults : Quantitative mechanistic study using the KCNQ1 mutation Q357R as example," *HRTHM*, vol. 9, no. 2, pp. 275–282, 2012.

[24] E. Grandi, F. S. Pasqualini, and D. M. Bers, "A novel computational model of the human ventricular action potential and Ca transient," *J. Mol. Cell. Cardiol.*, vol. 48, no. 1, pp. 112–121, 2010.

[25] T. R. Shannon, F. Wang, J. Puglisi, C. Weber, and D. M. Bers, "A mathematical treatment of

integrated Ca dynamics within the ventricular myocyte," *Biophys. J.*, vol. 87, no. 5, pp. 3351–3371, 2004.

[26] T. Hund and Y. Rudy, "Rate Dependence and Regulation of Action Potential and Calcium Transient in a Canine Cardiac Ventricular Cell Model," *Circulation*, vol. 110, no. 20, pp. 3168–3174, 2004.

[27] K. F. Decker, J. Heijman, J. R. Silva, T. J. Hund, and Y. Rudy, "Properties and ionic mechanisms of action potential adaptation , restitution , and accommodation in canine epicardium," vol. 4899, 2019.

[28] T. O. Hara and R. Schuessler, "Simulation Of The Undiseased Human Cardiac Ventricular Action Potential : Model Formulation , Experimental Validation And Application," *All Theses Diss.*, no. 873, 2011.

[29] H. C. Gadeberg, S. M. Bryant, A. F. James, and C. H. Orchard, "Altered Na/Ca exchange distribution in ventricular myocytes from failing hearts," *Am. J. Physiol. Circ. Physiol.*, vol. 310, no. 2, pp. H262–H268, 2016.

[30] C. Y. Zhao, J. L. Greenstein, R. L. Winslow, and T. Johns, "Roles of phosphodiesterases in the regulation of the cardiac cyclic nucleotide cross-talk signaling network," *J Mol Cell Cardiol*, vol. 91, pp. 215–227, 2017.

[31] T. J. Kamp and J. W. Hell, "Regulation of Cardiac L-Type Calcium Channels by Protein Kinase A and Protein Kinase C," 2000.

[32] X. Chen *et al.*, "Reduced effects of BAY K 8644 on L-type Ca2+ current in failing human cardiac myocytes are related to abnormal adrenergic regulation," *AJP Hear. Circ. Physiol.*, vol. 294, no. 5, pp. H2257–H2267, 2008.

[33] V. Piacentino *et al.*, "Cellular basis of abnormal calcium transients of failing human ventricular myocytes," *Circ. Res.*, vol. 92, no. 6, pp. 651–658, 2003.

[34] S. Bryant *et al.*, "Stimulation of ICaby basal PKA activity is facilitated by caveolin-3 in cardiac ventricular myocytes," *J. Mol. Cell. Cardiol.*, vol. 68, pp. 47–55, 2014.

[35] S. Wei *et al.*, "T-tubule remodeling during transition from hypertrophy to heart failure," *Circ. Res.*, vol. 107, no. 4, pp. 520–531, 2010.

[36] L.-S. Song *et al.*, "Orphaned ryanodine receptors in the failing heart," *Proc. Natl. Acad. Sci. USA*, vol. 103, no. 11, pp. 4305–4310, 2006.

[37] M. Kawai, M. Hussain, and C. H. Orchard, "Excitation-contraction coupling in rat ventricular myocytes after formamide-induced detubulation," *Am. J.* …, vol. 277, no. 2 Pt 2, pp. H603-609, 1999.

[38] M. M. Elshrif, P. Shi, and E. M. Cherry, "Representing Variability and Transmural Differences in a Model of Human Heart Failure," *IEEE J. Biomed. Heal. Informatics*, vol. 19, no. 4, pp. 1308–1320, 2015.

[39] D. Lang *et al.*, "HHS Public Access," vol. 8, no. 2, pp. 409–419, 2015.

[40] G. X. Liu *et al.*, "Differential conditions for early after-depolarizations and triggered activity in cardiomyocytes derived from transgenic LQT1 and LQT2 rabbits," *J. Physiol.*, vol. 590, no. 5, pp. 1171–1180, 2012.

[41] T.-T. Hong *et al.*, "BIN1 is reduced and Cav1.2 trafficking is impaired in human failing cardiomyocytes," *Hear. Rhythm*, vol. 9, no. 5, pp. 812–820, May 2012.

[42] X. Chen, V. Piacentino, S. Furukawa, B. Goldman, K. B. Margulies, and S. R. Houser, "L-type Ca2+ channel density and regulation are altered in failing human ventricular myocytes and recover after support with mechanical assist devices," *Circ. Res.*, vol. 91, no. 6, pp. 517–524, 2002.

[43] T. O'Hara, L. Virág, A. Varró, and Y. Rudy, "Simulation of the Undiseased Human Cardiac Ventricular Action Potential: Model Formulation and Experimental Validation," *PLoS Comput. Biol.*, vol. 7, no. 5, p. e1002061, May 2011.

[44] A. V. Glukhov *et al.*, "Transmural Dispersion of Repolarization in Failing and Nonfailing Human Ventricle," *Circ. Res.*, vol. 106, no. 5, pp. 981–991, Mar. 2010.

[45] J. D. Bayer, R. C. Blake, G. Plank, and N. A. Trayanova, "A novel rule-based algorithm for assigning myocardial fiber orientation to computational heart models," *Ann. Biomed. Eng.*, vol. 40, no. 10, pp. 2243–2254, Oct. 2012.

[46] E. J. Vigmond, R. Weber dos Santos, A. J. Prassl, M. Deo, and G. Plank, "Solvers for the cardiac bidomain equations," *Prog. Biophys. Mol. Biol.*, vol. 96, no. 1–3, pp. 3–18, Jan. 2008.

[47] E. J. Vigmond, F. Aguel, and N. A. Trayanova, "Computational techniques for solving the bidomain equations in three dimensions," *IEEE Trans. Biomed. Eng.*, vol. 49, no. 11, pp. 1260–1269, Nov. 2002.

[48] J. N. Weiss, A. Garfinkel, H. S. Karagueuzian, P.-S. Chen, and Z. Qu, "Early afterdepolarizations and cardiac arrhythmias," *Hear. Rhythm*, vol. 7, no. 12, pp. 1891–1899, Dec. 2010.

[49] G. S. Pitt, W. Dun, and P. A. Boyden, "Remodeled cardiac calcium channels," *J. Mol. Cell. Cardiol.*, vol. 41, no. 3, pp. 373–388, 2006.

[50] A. Hudmon, H. Schulman, J. Kim, J. M. Maltez, R. W. Tsien, and G. S. Pitt, "CaMKII tethers to L-type Ca2+ channels, establishing a local and dedicated integrator of Ca2+ signals for facilitation," *J. Cell Biol.*, vol. 171, no. 3, pp. 537–547, 2005.

[51] M. D. Fuller, M. a Emrick, M. Sadilek, T. Scheuer, and W. A. Catterall, "Molecular Mechanism of Calcium Channel Regulation in the Fight-or-Flight Response," *Sci. Signal.*, vol. 3, no. 141, pp. ra70-ra70, Sep. 2010.

[52] Y. S. Han, J. Arroyo, and O. Ogut, "Human heart failure is accompanied by altered protein kinase A subunit expression and post-translational state," *Arch. Biochem. Biophys.*, vol. 538, no. 1, pp. 25–33, 2013.

[53] F. Brette and C. Orchard, "T-tubule function in mammalian cardiac myocytes," *Circ. Res.*, vol. 92, no. 11, pp. 1182–1192, 2003.

ABBREVIATIONS

HF	heart failure
T-tubule	transverse tubule
LTCC	L-type calcium channels
P_o	open probability
PKA	protein kinase A
CAMKII	calcium-calmodulin kinase II
β_2AR	β_2 adrenergic receptor
AC	adenylyl cyclase
cAMP	cyclic adenosine monophosphate
AP	action potential
EAD	early afterdepolarization
DAD	delayed afterdepolarization
SA node	sinoatrial node
AV node	atrioventricular node
SR	sarcoplasmic reticulum

RyR	ryanodine receptor
NCX	Na^+/Ca^{2+} exchanger
CICR	Ca^{2+} - induced Ca^{2+} release
NaK	Na^+/K^+ pump
ICM	ischemic cardiomyopathy
DCM	dilated cardiomyopathy

SYMBOLS

V_m	transmembrane potential
I_{CaL}	L-type Ca^{2+} current
I_{K1}	inward rectifier K^+ current
I_{Kr}	delayed rectifier K^+ current
I_{NaCa}	Na^+/ Ca^{2+} exchanger (NCX) current
I_{NaK}	Na^+ / K^+ pump current
I_{NaL}	late Na^+ current
I_{Na}	fast Na^+ current
I_{to}	transient outward K^+ current

Vita

Alex Loucks was born on February 22nd, 1992 in Bucharest, Romania. She received her Bachelor of Science in Computer Science and Biochemistry and Molecular Biology from University of Richmond in 2015, and in the same year enrolled in the Biomedical Engineering Ph. D. program at Johns Hopkins University. As an undergraduate, Alex worked for 4 years in an organic chemistry synthesis lab, while during her graduate studies she was part of the Computational Cardiology Lab.

She received the David C. Gakenheimer Fellowship Award in 2016, 2017 and 2018. In her research, Alex focused on developing single-cell ventricular myocyte models that will help uncover the mechanisms linking microstructural remodeling to arrhythmias in patients suffering from hear failure. Starting in January 2019, Alex will work as a Software Engineer at Capital One Bank.